

Designing a Wireless Underwater Optical Communication System

by

Heather Brundage

B.S. Ocean Engineering
Massachusetts Institute of Technology, 2006

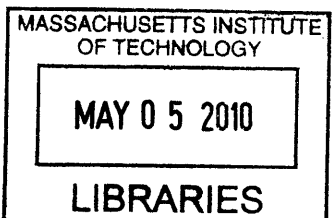
Submitted to the Department of Mechanical Engineering in
Partial Fulfillment of the Requirements for the Degree of

Master of Science in Mechanical Engineering

at the
Massachusetts Institute of Technology

February 2010

ARCHIVES



© February 2010 Heather Brundage. All rights reserved.

The author hereby grants to M.I.T. permission to reproduce and to distribute publicly
paper and electronic copies of this thesis document in whole or in part in any way now
known or hereafter created.

Signature of Author

Department of Mechanical Engineering
January 15, 2010

Certified by.....

Chryssostomos Chryssostomidis
Director, MIT Sea Grant College Program
Doherty Professor of Ocean Science and Engineering
Professor of Mechanical and Ocean Engineering
Thesis Advisor

Accepted by.....

David E. Hardt
Chairman, Department Committee on Graduate Studies

Designing a Wireless Underwater Optical Communication System

by

Heather Brundage

Submitted to the Department of Mechanical Engineering
on January 15, 2010, in partial fulfillment of the requirements
for the degree of
Master of Science in Mechanical Engineering

Abstract

Though acoustic modems have long been the default wireless communication method for underwater applications due to their long range, the need for high speed communication has prompted the exploration of non-acoustic methods that have previously been overlooked due to their distance limitations. One scenario that drives this need is the monitoring of deep sea oil wells by AUVs that could be stationed at the well and communicate surveillance data wirelessly to a base station. In this thesis, optical communication using LEDs is presented as an improvement over acoustic modems for scenarios where high speed, but only moderate distances, is required and lower power, less complex communication systems are desired. A super bright blue LED based transmitter system and a blue enhanced photodiode based receiver system were developed and tested with the goal of transmitting data at rates of 1 Mbps over distances of at least 10 meters. Test results in a fresh water tow tank showed the successful transmission of large data files over a distance of 13 meters and at transmission rates of at least 3 Mbps. With an improved test environment, even better performance may be possible.

Thesis Supervisor: Chryssostomos Chryssostomidis
Title: Director, MIT Sea Grant College Program
Doherty Professor of Ocean Science and Engineering
Professor of Mechanical and Ocean Engineering

Acknowledgments

This work was supported by a National Defense Science and Engineering Graduate fellowship, in connection with the Office of Naval Research, as well as the MIT Sea Grant Collage program. Without their support, this project would not have been possible.

I would like to thank my advisor, Dr. Chrys Chryssostomidis, for giving me the support and freedom to explore fun and challenging projects.

Dr. Milica Stojanovic for being my unofficial advisor and consultant on all things communications-related.

Professor Steve Leeb, and his knowledgeable grad students, for generously contributing their time and resources to assist me in the design of the optical transmitter.

“The boys” of the AUV Lab (Justin Eskesen, Ian Katz, Seth Newburg, Mike Soroka) and Sarah Hammond for helping me in so many aspects of this project, putting up with my clutter and providing camaraderie.

Janice Ahern, Nancy Adams, Trudi Walters and Kathy de Zengotita for handling all the logistics, accounting, scheduling, and other innumerable pieces of the puzzle that made this project possible and couldn’t have happened without them!

Norman Farr for a mid-thesis sanity check.

Alex Hornstein for late nights coding, a sympathetic ear, and providing me with the right tools for the job.

Friends and family for their support and encouragement.

and Michael Davis for reading through thesis drafts every day for a month, being a troubleshooting expert, making sure I didn’t drown in the tow tank, helping with circuit board layouts, making fantastic suggestions, keeping me company on late nights and long weekends in lab, providing immeasurable emotional support, and, in general, helping me and this project arrive at the finish line in good, working order.

List of Figures

Figure 1 Absorption coefficient of electromagnetic radiation at various wavelength (8)	11
Figure 2 Absorption coefficients of visible light wavelengths (9)	11
Figure 3 Wireless optical communication system overview	13
Figure 4 Transmitter System Overview	14
Figure 5 LED Schematic.....	15
Figure 6 Laser diode diagram (24).....	16
Figure 7 Titan™ Series LED Lighting System (11).....	19
Figure 8 Signal beam width of LEDs with the narrow beam (11°) lens at various distances.	20
Figure 9 MOSFET schematic diagram	21
Figure 10 Transmitter schematic	22
Figure 11 Channel 1 (bottom trace) shows the MOSFET gate voltage when being driven directly from a signal generator producing a 0-5 V square wave.	23
Figure 12 Channel 2 (blue trace) in both (a) and (b), which is zoomed in, show the MOSFET gate being driven by an IR2151 which is receiving a square wave signal from a signal generator (Channel 1, orange).	24
Figure 13 Channel 2 (blue trace) shows MOSFET gate voltage being driven by the TC4427 MOSFET driver.....	24
Figure 14 TTL232R USB-TTL Level Serial Converter Cable from FDTI	25
Figure 15 Schmitt inverter and truth table (31)	26
Figure 16 Transmitter system	26
Figure 17 Testing the transmitter design.	27
Figure 18 Oscilloscope test probe locations for the subsequent screen grabs.	28
Figure 19 Initial transmitter tests	28
Figure 20 Improved transmitter testing.....	29
Figure 21 Wire-wound (a) vs. Ceramic (b) current-limiting resistors	30
Figure 22 Final breadboard testing, the blue disks are 1 ohm ceramic resistors.	30
Figure 23 Final transmitter testing with inverter added to the PCB	31
Figure 24 Transmitter PCB mechanical layout.....	32
Figure 25 Populated transmitter printed circuit board	32
Figure 26 Receiver system diagram.....	33
Figure 27 Photoresistor symbol	33
Figure 28 Photothyristor symbol	34
Figure 29 Phototransistor symbol	34
Figure 30 Picture of a photomultiplier (20)	35
Figure 31 Spectral response of various photodiodes (39).....	38
Figure 32 PC10-6B	38
Figure 33 Receiver electrical system diagram	39
Figure 34 Basic passive current-to-voltage converter	40
Figure 35 Transimpedance Amplifier.....	41
Figure 36 Transimpedance amplifier feedback resistor testing	42
Figure 37 Output of transimpedance amplifier when C_f is too large.....	43
Figure 38 Tuning C_f (a) C_f too small (b) C_f just right (c) C_f too large.....	43
Figure 40 Comparing two different voltage amplifiers (a) LM318 (b) LM7171	44
Figure 39 Inverting amplifier.....	44

Figure 41 Comparator input (top) vs output (bottom)	46
Figure 42 Op-Amp Comparator Schematic	46
Figure 43 Receiver breadboard testing	47
Figure 44 Ringing is present in the receiver circuit while testing on the breadboard.	47
Figure 45 Receiver printed circuit board layout	48
Figure 46 Back side of the receiver printed circuit board with components	48
Figure 47 Receiver testing with the PCB (a) 1 Mbps (b) 3 Mbps	49
Figure 48 Water testing set up	50
Figure 49 Transmitter water test set-up	51
Figure 50 Receiver water testing mount.....	52
Figure 52 Complete receiver test set-up	53
Figure 51 Semi-submerged receiver mounted in the tank	53
Figure 53 Aligning the transmitter and receiver	54
Figure 54 Testing sending/receiving capabilities without the optical link	55
Figure 55 30 KB JPEG file transmitted through cable (a) 1 Mbps (b) 2 Mbps (c) 3 Mbps	56
Figure 56 Graph of received signal strength at various transmission distances	56
Figure 57 Received data at 1 Mbps over 13 meters.....	57
Figure 58 Testing at the distance limits of the system (a) 15 meters (b) 16.2 meters	58
Figure 59 (a) Original file (b) transmitted at 1 Mbps and (c) 3 Mbps over the optical link.....	58
Figure 60 Received data signal at (a) 1 Mbps (b) 2 Mbps (c) 3 Mbps	59
Figure 61 Bubbles on the face of the glass in front of the transmitter.....	59

List of Tables

Table 1 Comparison of various underwater acoustic modems (4)(5)(6)	10
Table 2 Comparison of LEDs and Laser Diodes (21)(23)(20)(22)(24)(25)	17
Table 3 A comparision of high-powered LEDs on the market.....	18
Table 4 Comparison of photodetectors (34)(20)(19)(36)	37

Table of Contents

1	Introduction.....	7
2	Background	9
2.1	Wireless Communication Methods	9
2.1.1	Acoustics.....	9
2.1.2	Electromagnetic Waves	10
2.2	Design Constraints	12
3	System Design	13
3.1	Optical Transmitter	14
3.1.1	Photon Source.....	15
3.1.2	LED Driver	20
3.1.3	Data Signal.....	25
3.1.4	Testing the Transmitter System	26
3.1.5	Finalizing the Transmitter System	30
3.2	Optical Receiver.....	33
3.2.1	Photon Detector	33
3.2.2	Signal Processing.....	39
3.2.3	Receiver Testing	46
4	System Water Testing	49
4.1	Setup.....	49
4.1.1	Transmitter.....	50
4.1.2	Receiver	52
4.1.3	Alignment	54
4.2	Testing.....	54
4.3	Results	56
5	Conclusion	60
6	Bibliography	61
	Appendix.....	64

1 Introduction

A major driver of technology is to create machines that can perform tasks in place of humans. Whether the task is too repetitive and boring, requires more precision, or is too dangerous for a person to perform, a robotic system can provide the solution. Though people are no longer able to, or no longer wish to, perform a task, the state of artificial intelligence has not progressed to a point where people are comfortable being completely removed from the loop. Robotic operators still need to communicate with their machines to various degrees – sometimes to completely control them, other times to monitor progress or review data collected from sensors.

The easiest technological way to communicate with a robot is through a physical connection, such as a copper or fiber optic tether. Though this allows for efficient and high-speed communication, a tether provides many operational challenges when dealing with a mobile robot, limiting the range and maneuverability of the vehicle, as well as requiring an often cumbersome tether management system. For these reasons, wireless communication is a much more feasible solution to the problem of communicating with robotic vehicles. In aerial and terrestrial applications, radio and satellite communications provide adequate speed and range. Underwater environments, on the other hand, have a much greater challenge in achieving wireless communication, while at the same time requiring wireless communication even more.

Since humans are limited in their ability to work underwater, remotely operated vehicles (ROVs) and autonomous underwater vehicles (AUVs) have been in service since the 1950's (1)(2) to perform underwater tasks, such as collecting data and retrieving items. Operation of these vehicles is challenging, but as oil resources are found further off shore, ROVs and AUVs are required to go deeper and stay deployed longer in order to perform critical tasks. One such task is monitoring a deep sea oil well - sending tethered ROV's thousands of meters below the surface in order to conduct surveys is expensive and time consuming! It costs on the order of \$100,000 a day to operate an ROV, which can take two hours to dive to the bottom at 3000 meters. This hefty price tag is due to the many expenses including the cost of the boat, the crew, the ROV, and the ROV support team.

A cheaper alternative is to remove the boat and crew from the equation by leaving an AUV stationed at the well, able to charge and communicate with the surface and monitor the well as needed. This would greatly reduce the operational costs involved with current well monitoring and be a much more time and resource efficient approach. In this scenario, a tethered connection between the base station and the AUV would greatly limit the AUVs ability to maneuver. On the other hand, any sort of docking situation requiring a wet-mateable connection would degrade rapidly after hundreds cycles, making it unreliable for long term deployment. In this case, wireless data transfer is required to provide the cost saving benefits of stationing an AUV at a well head. The wireless communication method must be able to support data rates high enough to upload video and other sensor data. Thankfully, long distances are not required, since the AUV could dock or hover anywhere from .1-10 meters from the base station. Power usage and overall size need to be taken into consideration, since the AUV will be running off batteries.

In this paper, I will present a solution to the need for low-power, cost effective, high-speed wireless communication. In the next section, I will compare possible wireless communication methods, present an overview of past work in this area, and cover necessary background information. In the third section, I will present my design and the rationale behind key decisions. In the fourth section I will present data from system tests and in the fifth section I will review the system performance.

2 Background

2.1 Wireless Communication Methods

There are two main mediums by which data can be transmitted wirelessly – acoustic waves and electromagnetic waves. Both of these are used extensively in terrestrial applications. Humans take advantage of wireless acoustic transmission when speaking to one another, while radios work thanks to electromagnetic transmission. In the next few sections, I will discuss how these methods are suited for underwater wireless communication.

2.1.1 Acoustics

Though sound travels decently through air, it travels much better through water. The speed of sound in water is about 1500 m/s, compared to the approximately 340 m/s it travels in air. But the speed at which sound travels through water is highly dependent on the temperature, pressure and salinity of the water. As a result, the presence of thermoclines (temperature gradients) and haloclines (salinity gradients) in the ocean cause acoustic waves to refract when encountering these boundaries. This can drastically change the direction the sound is moving in, or even channel the sound and propagate it long distances (thousands of meters).

Though some sounds can travel remarkable distances, higher frequency sound is attenuated much faster than lower frequency sound (3). This presents a trade-off between communication speed (high frequency acoustic signals allow for higher data transfer rates) and distance (lower frequency acoustic signals can travel further). This can be seen in Table 1, which compares various acoustic modems. A general trend is obvious in the table: as distance increases, data rate and transmission frequency go down, while size and power increase.

You can see from the table that the fastest acoustic modems can only transmit at data rates of less than a couple hundred kilobits per second. Though this works okay for commands, it is too slow to deal with video. Also, since sound propagates so well underwater, it means there can be a lot of acoustic “noise” in the channel, making it harder to receive a clean signal that doesn’t get lost in the noise. This is especially true at deep sea well heads which can be very noisy. Though acoustic modems have their uses and are the only way to send a wireless signal long distances

underwater, acoustic wireless transmission is not ideal for this application which requires high speeds over short distances.

Model	Distance (m)	Data Rate (kbps)	Center Frequency (kHz)	Power (Watts)	Weight in Air (kg)
Link Quest UWM1000	350	17.8	35	1	4.2
Link Quest UWM2000	1500	17.8	35	4	5.1
Link Quest UWM3000	3000	5	10	12	6.7
LinkQuest UWM4000	4000	8.5	17	7	8.2
HERMES	120	150	310	32	
Evo Logics S2C R 48/78	2000	28	63	80	6.5
Evo Logics S2C R 40/80	2500	33	65	80	6.5
Evo Logics S2C R 18/34	4500	14	24	80	6.5
Evo Logics S2C R 12/22	8000	10	17	80	7.4
Evo Logics S2C R 8/16	10000	6.5	12	80	7.8

Table 1 Comparison of various underwater acoustic modems (4)(5)(6)

2.1.2 Electromagnetic Waves

A much faster communication medium is electromagnetic waves. These waves travel at the speed of light, $\sim 300,000,000$ meters/second, which is about 200,000 times faster than sound travels through water! Electromagnetic waves are also unaffected by salinity, temperature and depth. Unfortunately, all electromagnetic waves are highly attenuated in water, meaning the signal cannot go very far. This is due to both absorption and scattering. Figure 1 shows the absorption of different wavelengths. You can see that blue optical light is attenuated the least of all electromagnetic radiation. The exact wave length that penetrates the furthest through sea water depends on the characteristics of the specific water, since absorption and scattering is influenced by the chemical and biological make up of the water, but in general wave lengths in the 470nm range are attenuated the least (7). You can see this in Figure 2, which shows the same data as in Figure 1, but zoomed in to only the visible light spectrum.

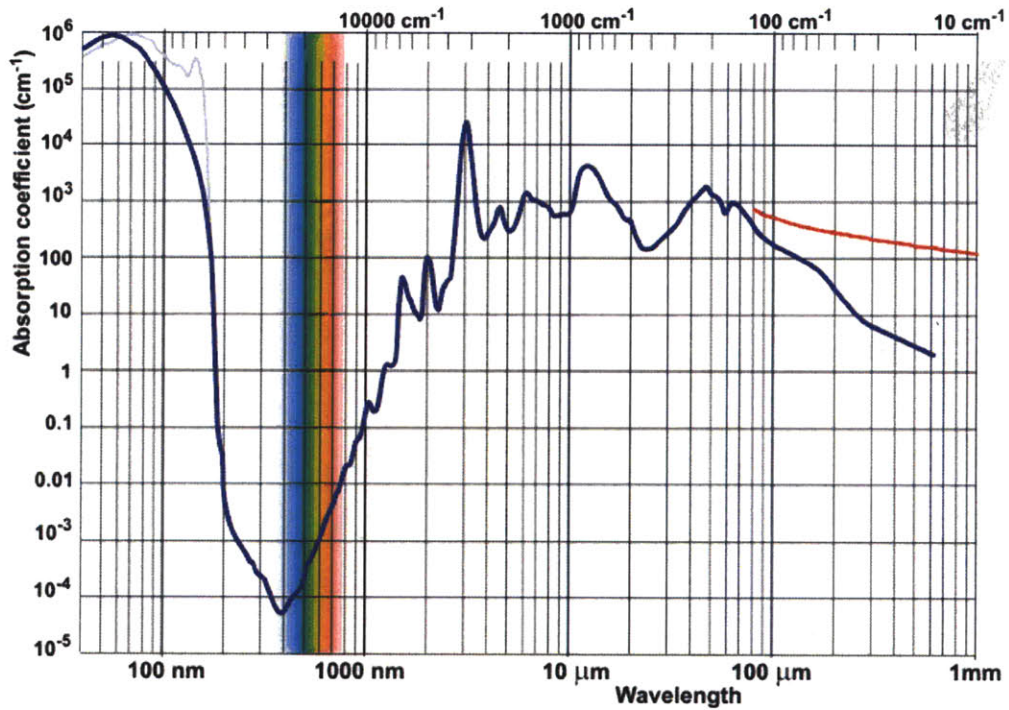


Figure 1 Absorption coefficient of electromagnetic radiation at various wavelength (8)

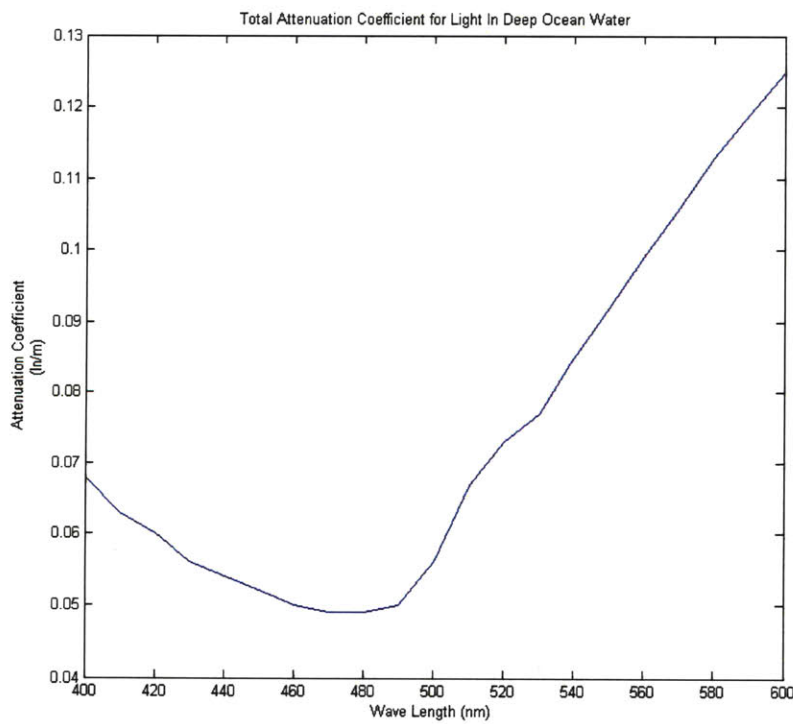


Figure 2 Absorption coefficients of visible light wavelengths (9)

Even though blue visible light propagates the furthest in sea water, some people have tried using radio waves for wireless underwater communication. RF communications require large and specially designed antennas, above or below water. Wireless Fibre is one company that is currently selling wireless RF underwater systems which they claim can transmit data at 100 kbps over tens of meters (10). Though there are situations where RF communication could be beneficial, the speeds are still too slow for this application and the required antenna size is too large.

Noticing the dip in absorption illustrated in Figure 2, many people have explored using blue light to wirelessly transmit data underwater. In 1995, Bales and Chryssostomidis proposed LED wireless underwater optical communications systems that could theoretically transmit 10 Mbps over a range of 20 meters or 1 Mbps over a range of 30 meters (11). Giles and Bankman take that further in 2005 by calculating theoretical transmission distances for 220 kbps and 4.4 Mbps data rates in various types of water, suggesting the range can vary from less than 10m to over 25m (12). In 2006, Farr et al did preliminary testing with an omni-directional LED communication system and extrapolated to hypothesize that in the future, 10 MHz transmissions could be possible over distances of 100 meter (13). Using lasers instead of LEDs, Hanson and Radic demonstrated 1 Gbps communication over 2 meters in a laboratory water pipe in 2007 (14) and a commercial company, Ambalux Corporation, currently sells a laser-based optical communication system they claim can transmit at 10Mbps over 40 meters (15).

In optimizing for specific design criteria, other researchers have demonstrated impressive results in communication distance and speed. Many have reported transmission speeds in the hundreds of kilobits per second range, over distances of up to five meters (16)(17). More recently, Doniec et al reported 1.2Mbps transmission over 30 meters (18).

2.2 Design Constraints

The previous research shows that underwater wireless optical communication could be a viable solution to the problem of an AUV needing to communicate with a base station at a deep sea oil well head. However, this scenario does impose some specialized design constraints on the system. Mainly, that the system will need to be integrated into a space- and power-limited AUV.

This means that the system needs to use minimal power and take up minimal space. It also means that the system needs to work even without perfect alignment of the transmitter and receiver, since the hovering AUV cannot hold a position without some margin of error. Since the AUV will be deployed and therefore not easily accessible by repair and maintenance crews for a long period of time, a simple system that requires little to no maintenance and has a minimal probability of failure is preferred. Finally, the communication system needs to be high speed (≥ 1 Mbps) and transmit as far as possible. These priorities – high speed, low power, small size, low complexity, and maximum distance – are what must drive the system design.

3 System Design

A wireless optical communication system is made up of a couple key components (see Figure 3). The computer (be it a laptop or a microprocessor) sends data to the transmitter which converts the electrical signal into an optical signal. That signal passes through the transmission medium (in this case, water) and is picked up by the receiver. The receiver detects the optical signal, converts it back into an electrical signal and passes that data back to the receiving computer.



Figure 3 Wireless optical communication system overview

There are many different ways light can carry data, but the simplest way is called on-off keying (OOK). In OOK, a binary one is represented as the light being on, and a binary zero is represented by the light being off. This means that the transmitter must be able to read in binary data and quickly and accurately change the state of the optical component accordingly. On the

other end, the receiver use a photodetector to determine if the light is on or off and outputs binary ones and zeros accordingly. The speed and reliability of the system is determined by how fast the transmitter can switch the state of the optical component and how quickly and accurately the receiver can determine the state of the light. In the following section, I will describe each subsystem in detail.

3.1 Optical Transmitter

The optical transmitter converts the electrical data signal into an optical signal and projects that optical signal into the transmission channel. It consists of the photon source, which acts as the electro-optical converter, as well as auxiliary systems required to operate and condition the photon source. Figure 4 shows a typical optical transmitter consisting of the input signal, the optical driver system, the photon source, and any light-beam conditioning optics required, such as reflectors and lenses.

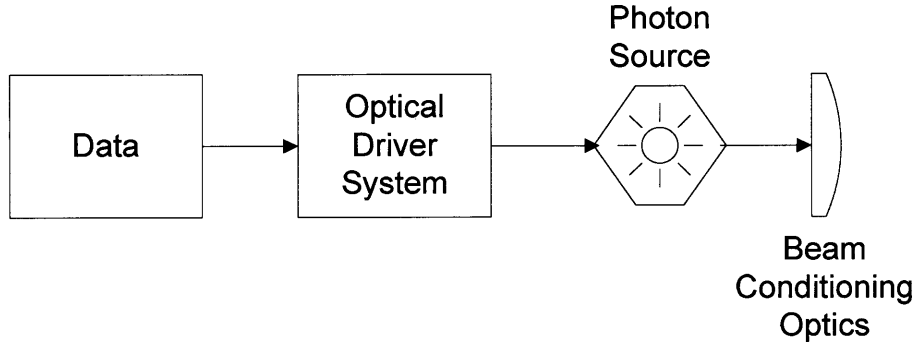


Figure 4 Transmitter System Overview

When designing an optical transmitter, the first step is to decide on your photon source, as the rest of the transmitter is designed to support the selected photon source. In order to determine the best photon source for a system, the available sources must be compared in terms of the goals and constraints on the system, as described in section 2.2.

3.1.1 Photon Source

Selecting the photon source drives the design of the rest of the optical transmitter. Though any photon source, from an incandescent lamp to a laser, could be used, the size, power and switching speed constraints placed on the system narrowed down the selection to two feasible choices: light emitting diodes (LEDs) and laser diodes (LDs). As is to be expected, there are tradeoffs between switching speed, system complexity, and system cost.

3.1.1.1 Light Emitting Diodes (LEDs)

Light emitting diodes (LEDs) are *pn*-junction semiconductors that emit visible or infrared light when forward biased – when the anode is more positive than the cathode (see schematic in Figure 5). Like regular *pn*-junction diodes, LEDs are made from *n*-type (negative) and *p*-type (positive) silicon joined together so that excited electrons on the *n* side can cross the *pn*-junction to combine with holes on the *p* side. The difference is that LEDs are designed in such a way that when electrons combine with holes, they release their energy as emitted photons (19). This random recombination creates spontaneous emission, which emits incoherent light, meaning the photons do not have a constant phase relation (20). Additionally, since photons are released only when electrons recombine with holes, if more electrons and holes recombine, then more photons are released. This means that light output of LEDs is linearly proportional to the drive current.

Unlike incandescent bulbs, which give off many wavelengths of light thereby producing white light, LEDs emit specific colors of light. The wavelength of the emitted photons (the color of light emitted) is determined by the band gap of the semiconductor. The width of the output spectrum (the variation in the wavelengths emitted) can vary upwards of 50nm around that center wavelength dictated by the band gap. Since water absorbs many wavelengths, it is beneficial to use a light source that only produces photons in the ~470 nm (blue light) range, as discussed in Section 2.

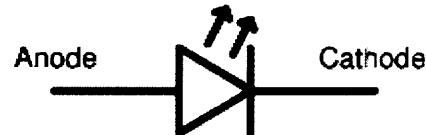


Figure 5 LED Schematic

The switching speed of an LED is determined by its recombination time constant. Depending on the design, the rise time can vary from 1 to 100ns (21), meaning LEDs can reach modulation speeds of up to hundreds of MHz.

Though LEDs are affected by extreme heat – they can become non-linear, reduce efficiency and even fail (20) – they are generally highly efficient, stable, and reliable light sources that have a long life time. Because of their simplicity and reliability, LEDs are relatively cheap and widely available.

3.1.1.2 Laser Diodes (LDs)

Laser diodes are similar to LEDs, in that they are built on pn-junctions (see Figure 6), but they are modified to allow the spontaneously emitted photons to cause other electron-hole pairs to recombine. These photon-induced recombinations emit photons with the same energy,

frequency and phase as the incident photon that caused them. This is called stimulated emission and results in coherent light. Stimulated emission occurs only after a threshold current has been reached. It has a much lower recombination time constant, and therefore laser diodes have a much faster rise time, allowing for modulation bandwidths in the GHz range (20). It also results in high optical power emissions in a very narrow optical spectrum width, around 1 nm (19).

Unfortunately, stimulated emission is challenging to maintain. Laser diodes are very sensitive to changes in temperature and current - the wavelength of the laser diode can change by about $0.1\text{nm}/^{\circ}\text{C}$ (22) and the efficiency and threshold current can change significantly due to age and temperature (20). Thermal, optical and electrical feedback is necessary to sustain operation and prevent the laser diode from failing. This adds complexity and cost to the system. The sensitivity of laser diodes results in shorter life times and lower reliability.

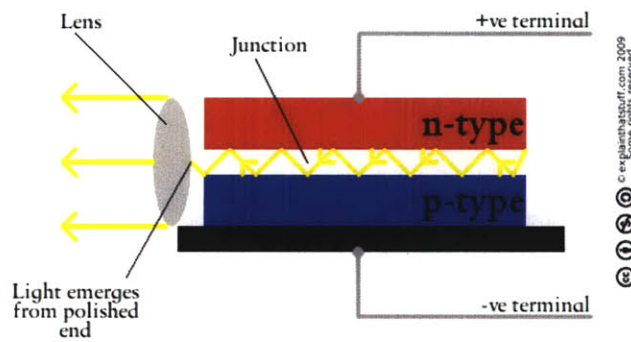


Figure 6 Laser diode diagram (24)

3.1.1.3 Photon Source Selection

As the previous sections have shown, the choice between LEDs and Laser Diodes is complicated. Table 2 gives an overview of the findings:

Characteristic	LED	Laser Diode
Optical Spectral Width	25-100 nm	.01 to 5 nm
Modulation Bandwidth	<200 MHz	> 1 GHz
Minimum Output Beam Divergence	Wide (about 0.5°)	Narrow (about 0.01°)
Temperature Dependency	Little	Very temperature dependant
Special Circuitry Required	None	Threshold and temperature compensation circuitry
Cost	Low, off-the-shelf components available	High, need specialized optics and electronics
Lifetime	Long, with little degradation of power levels	Medium, power levels degrade over time
Reliability	High, 10^8 hours	Moderate, 10^5 hours
Coherence	Incoherent	Coherent
Eye Safety	Eye safe	Must take precautions

Table 2 Comparison of LEDs and Laser Diodes (21)(23)(20)(22)(24)(25)

Both LEDs and laser diodes have strengths and weaknesses when it comes to underwater free space optical communications. Laser diodes can switch faster and have higher optical power output, but LED systems are cheaper, simpler, and more reliable. Though the coherence and minimal divergence of laser diodes is optimal for optical fiber communication systems, it does not play as big a role in wireless optical communication. Additionally, though laser diodes can switch faster, LEDs can switch fast enough for our application (≥ 1 MHz). Since the goal is to have a small, cheap, reliable communication system that can handle at least 1 MHz, LEDs were selected as the photon source for the optical transmitter.

3.1.1.4 LED Selection

Once the decision was made to use LEDs, the specific LED(s) needed to be selected. Since the goals are to be able to transmit the signal as far as possible, the maximum amount of optical power in the 470 nm range is needed. This can be accomplished by choosing super bright LEDs and by using multiple LEDs. With that in mind, many different LED manufacturers were researched to find the brightest blue (~470 nm) LED on the market. Table 3 shows a comparison of various high-power LEDs on the market (all data taken from their respective data sheets). You can see that high power LEDs can give off a luminous flux of 30-60 lumens. This is compared to the less than 1 lumen that standard LEDs produce. Though other colored LEDs, such as Amber, have been around for a long time and are able to produce upwards of 130 lumens per LED, blue LED technology is not as advanced and therefore has a lower lumen output.

Manufacturer and Model	Wave Length (nm)	Luminous Flux (lm)
Lamina Atlas NT-42C1-0484	460-470	63
AOP LED Corp PU-5WAS	455-475	54
Luxeon Rebel LXML-PB01-0023	460-490	48
Kingbright AAD1-9090QB11ZC/3	460	35.7
Ligitek LGLB-313E	460-475	30.6
Toshiba TL12B01(T30)	460	6
Lumex SML-LX1610USBC	470	5
Typical(not high-power) LED	470	< 1
High Powered Amber LED(26)	590	130

Table 3 A comparision of high-powered LEDs on the market

High power LEDs generally use 1-5 Watts of power and draw 700-1050mA current, meaning they require a forward voltage of 2-5 volts per LED in series, depending on the LED. In order to maximize light output, more LEDs are desirable, but this must be balanced with the power limitations placed on the system. In this case, the AUV that will carry the transmitter already has a 12 and 24 volt power supply, so it made sense to limit the number of LEDs used so that no more than 24 volts was needed to drive them. Additionally, as more LEDs are added, optical and thermal properties must be taken into account. Though LEDs are not nearly as sensitive to high

temperatures as laser diodes and do not require thermal monitoring, high power LEDs must still be attached to heat sinks to ensure they do not overheat. As more LEDs are added to the system, more or bigger heat sinks are required and all LEDs must be fully thermally coupled to the heat sink. Additionally, since each LED gives off its own light, optics must be used to focus the disparate beams into one beam.

In order to simplify the system and ensure proper operation, it was decided to look for an off-the-shelf lighting engine that incorporated multiple LEDs. Designing specialized optics and heat sinks was not in the scope of this project and the specialized tools necessary to ensure proper thermal coupling between the LEDs and the heat sinks were not available. Though many LED manufacturers make single LED chips, very few integrate them with heat sinks and lenses. Luckily, one company, Lamina Lighting, did just that, and had incredibly bright blue LEDs to boot. Their Titan™ Series LED Lighting System (see Figure 7) uses their Titan blue lighting engine (NT-52B1-0469), which has seven blue LEDs in series that typically provide 244 lumens at 1 amp and require 19.7 volts (27). It comes assembled with a heat sink, optics (lens and reflector) and wire harness.

The lens selection also comes down to a trade off. The wider the light beam angle, the less accurately the AUV must hold position while transmitting data. At the same time, the optical signal received is weakened as the beam is widened, since the optical power is spread over a larger area. System constraints, such as the ability of the AUV to hold position within a half meter radius of a specified point and the desire to send the signal as far as possible, rule out the extremes of a single beam of light (like a laser, since the AUV cannot hold a position that tightly while hovering) and an omni-directional light source (since the optical power would be spread



Figure 7 Titan™ Series LED Lighting System (11)

further, meaning the distance would be reduced). Additionally, only four lens choices are available for the Titan lighting system: narrow beam (11°), narrow (24°), medium beam (35°), and wide beam (48°). Figure 8 shows how far the beam would spread over 10 meters when using the narrow beam (11°) lens. As you can see, the AUV could hover as close as 2.5 meters away from the base station and still be able to maintain position well enough to complete a transmission. Since the narrow beam lens allowed the AUV to be an acceptable distance away without spreading the beam so far that optical power would be wasted, the narrow beam lens was chosen to be installed on the Titan lighting system.

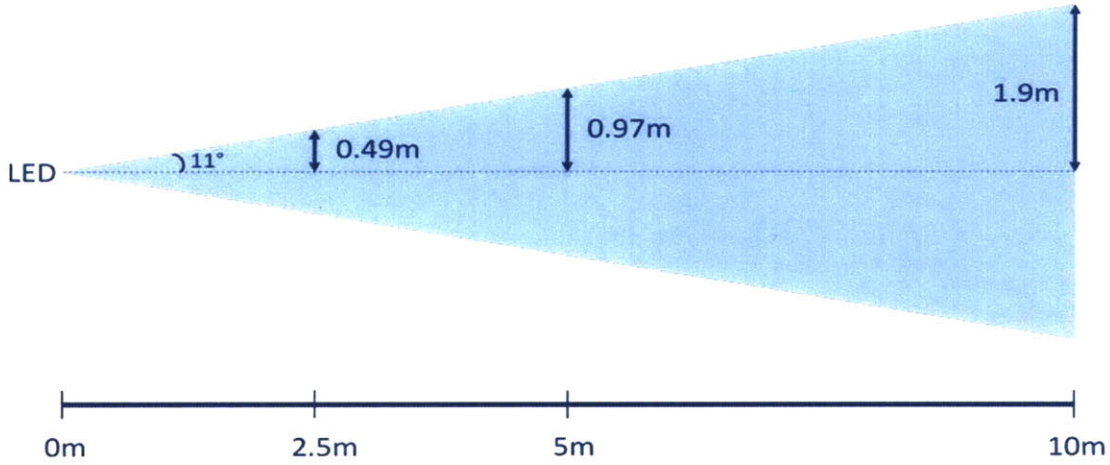


Figure 8 Signal beam width of LEDs with the narrow beam (11°) lens at various distances.

3.1.2 LED Driver

Once the light source was determined, the next step was to design a way to modulate it (turn it on and off) in correlation with the binary data. Since LEDs are current-controlled devices (their output is linearly related to the supply current), a constant current switching power supply would be ideal to maximize efficiency. These are challenging to design from scratch, but there are commercially available constant-current LED drivers. Unfortunately, these are designed for lower speed switching applications, such as LED dimming, and therefore are not optimized for the high speeds optical communications require. No commercial, off-the-shelf LED drivers could be found that could supply the required power (~20 Watts) at the desired speed (≥ 1 MHz).

An alternative way of controlling LEDs is to provide a constant voltage (much more common) and limit the current passing through the LEDs using resistors. In this situation, a transistor (an electronically controlled switch) can be used to start and stop the flow of current through the LEDs, turning them on and off. A metal oxide semiconductor field-effect transistor (MOSFET) is best suited for the job. MOSFETs (see schematic in Figure 9) consist of a drain, gate and source. When there is no voltage difference between the gate and the source, there is a very high resistance between the drain and the source so minimal current flows from the drain to the source – the MOSFET is “off”. If, however, the gate is supplied with a voltage, the drain-source channel becomes less resistive (19) – the MOSFET is “on”. Once the gate threshold voltage has been reached, the MOSFET is fully on and the only resistance between the drain and the source is the drain to source on resistance.

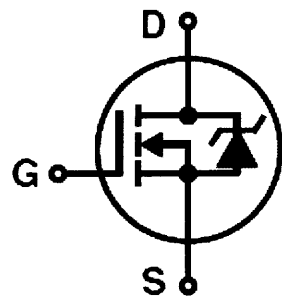


Figure 9 MOSFET schematic diagram

MOSFETs are better suited for this application compared to bipolar transistors because they have a much lower drain to source on resistance (milliohms as compared to 10-100 milliohms (19)). This means they will produce a smaller voltage drop and can handle larger currents. Additionally, MOSFETs are better than junction field-effect transistors (JFETs) because they have a much larger gate input impedance (10^{14} ohms compared to 10^9 ohms (19)). This means that they draw very little gate current. This is advantageous since the computer or integrated circuit (IC) sending the data signal to the MOSFET typically cannot source a lot of current. If the gate impedance were lower, more current would be needed to change the gate voltage.

Even though the gate impedance is high, there is also a gate capacitance. The larger the gate capacitance, the more current that is needed to charge the gate before the voltage will change. This means that the magnitude of the gate capacitance, and the amount of current that the incoming signal can source, greatly affects that switching speed of the MOSFET. For this reason, MOSFETs that need to switch high power loads very quickly (which is the case in design) often employ a MOSFET driver that takes in the data signal and is able to source significantly more current to the MOSFET gate.

There are different types of MOSFETs and MOSFET drivers. For this application, a MOSFET that could quickly switch more than 24 volts at 1 amp was necessary. This means it had to have a drain to source breakdown voltage of at least 50 V and minimal rise and fall time. Additionally, it had to be able to operate from TTL logic levels (0 volts = "0", 5 volts = "1"), which means the gate threshold voltage had to be below 5 volts. After comparing various MOSFETs, the 40N10 was selected. With a drain to source breakdown voltage of 100V and a maximum drain current of 40A, it could more than handle the power requirements of the LEDs. Additionally, its gate threshold voltage is between 2 and 4 volts and it has a very short rise time of 30 ns (28). The TC4427A was selected as the MOSFET driver since it could operate off the 12 V power rail and could drive a high capacitive load very quickly - 1000 pf in 25 ns (29).

Figure 10 shows the transmitter circuit schematic. The TTL data signal (0-5 V) goes into the TC4427A MOSFET driver which runs off the AUV's 12 volt power rail. The driver controls the MOSFET gate which, when on, allows current to flow through the LEDs and current-limiting resistors which are powered by the AUV's available 24 volt power rail. The 4 ohms of resistance limit the current that flows through the LEDs to 1 amp.

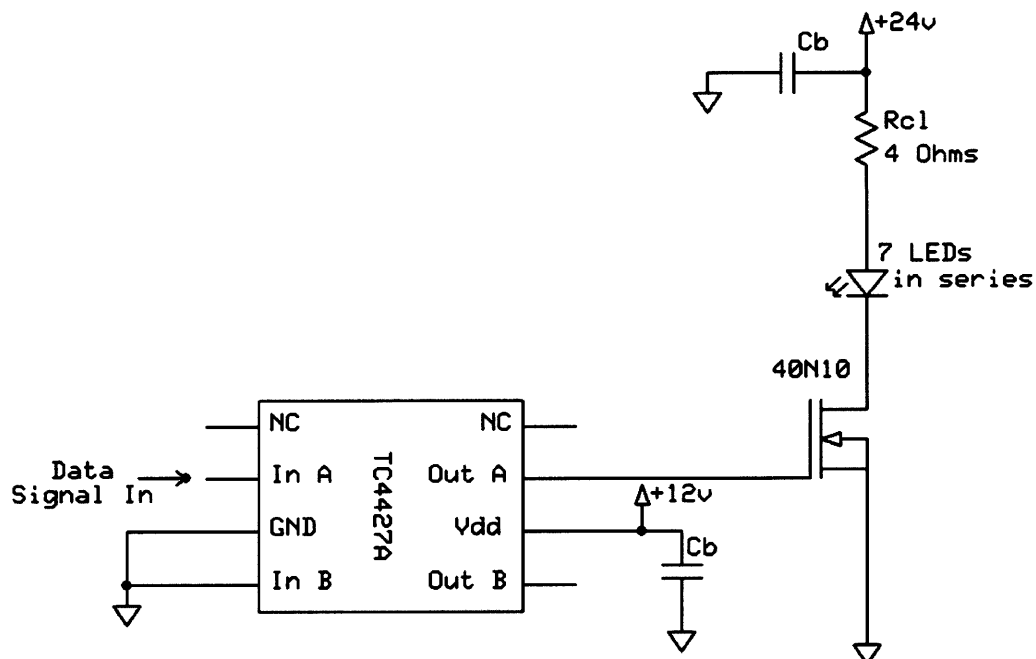


Figure 10 Transmitter schematic

The oscilloscope traces below help illustrate the importance of the MOSFET gate driver in the switching speed of the system. They show the difference between not using a MOSFET driver (Figure 11), using a decent one (Figure 12), and using a better one (Figure 13). Channel 1 (the bottom trace) in Figure 11 shows the voltage on the MOSFET gate when it is being driven directly by a signal generator providing a 400 kHz, 0-5V square wave.

Channel 2 (top trace) shows the drain of the MOSFET. You can see from the figure that it takes over 1 μ s for the MOSFET gate to reach the full 5 volts the signal generator is trying to drive it to. It is not until the gate voltage passes its threshold that the MOSFET is completely “on” (trace 2 goes to 0 V). While the gate ramps up and down over a period of more than 1 μ s, the MOSFET is partially on, allowing limited current through. You can see the results of this on trace 1 where the voltage slopes gently down to 0 volts and then slopes back up. This is undesirable, since it will affect the operation of the LEDs and the resulting optical signal.

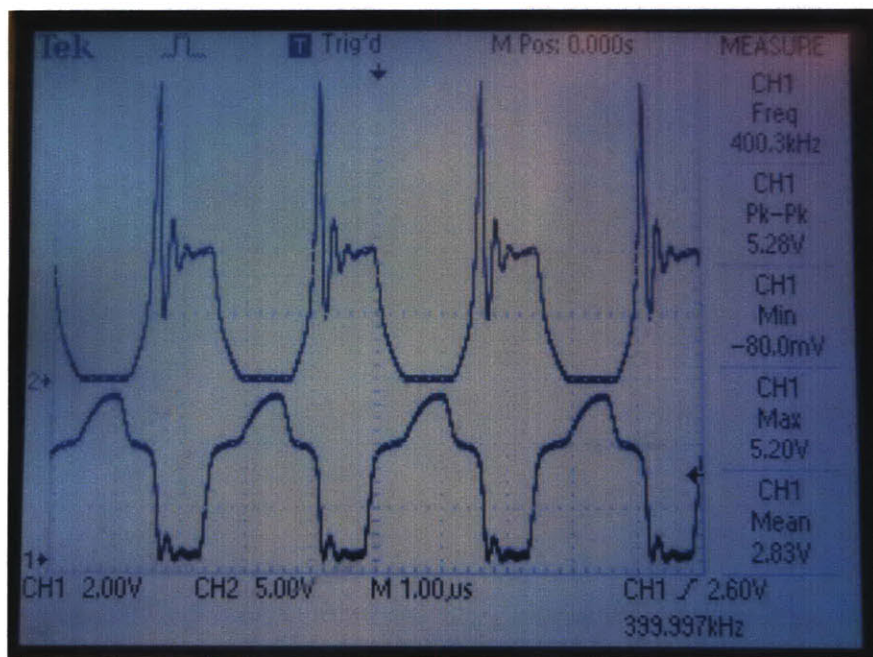


Figure 11 Channel 1 (bottom trace) shows the MOSFET gate voltage when being driven directly from a signal generator producing a 0-5 V square wave.

Channel 2 (the blue trace) in Figure 12 (a) and (b) shows the MOSFET gate voltage, but this time, the gate is being driven by an IR2125 MOSFET driver. The IR2125 is receiving a square wave from a signal generator (Channel 1, orange). In the figure, you can see that the gate voltage ramps up to the full signal voltage (in this case, 12 volts) in about 300 ns.

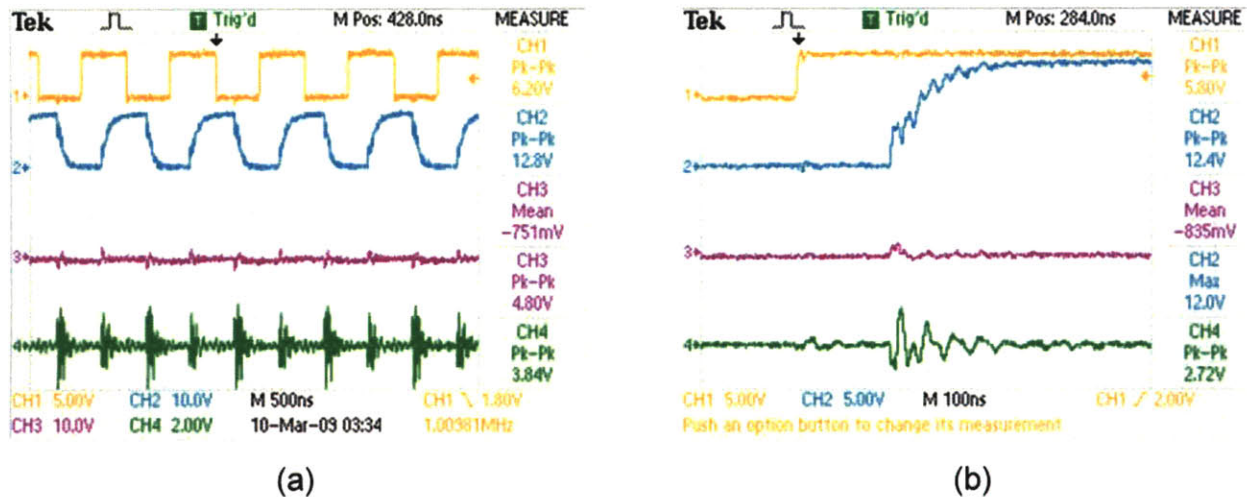


Figure 12 Channel 2 (blue trace) in both (a) and (b), which is zoomed in, show the MOSFET gate being driven by an IR2151 which is receiving a square wave signal from a signal generator (Channel 1, orange).

The last trace shows an upgrade from the IR2125 to the TC4427 MOSFET driver. This driver is slightly more powerful than the IR2125 and has a faster rise and fall time. As can be seen in Figure 13, the rise time of the MOSFET gate (trace 2, blue), while being driven by the TC4427, is about 200 ns. This is significantly faster than the 1 μ s it takes for the MOSFET gate to reach its full voltage with no driver. Additionally, you can see that the drain of the MOSFET (trace 3, purple) has a much better defined “on” and “off”, without that slow ramp up and down.

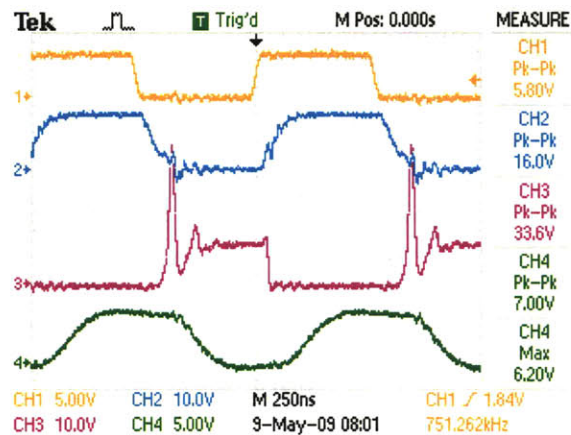


Figure 13 Channel 2 (blue trace) shows MOSFET gate voltage being driven by the TC4427 MOSFET driver.

3.1.3 Data Signal

Once the transmitter had been designed, a way was needed to get binary data from the computer delivered to the MOSFET driver in TTL levels (0 volts = “0”. +5 volts = “1”). The communication protocol used (hand shaking, initialization packets, etc) is irrelevant, since it will just be passed through the optical transmitter system and returned to binary data on the receiver end. The only issue is getting computer output data into TTL levels.

The computer on the AUV has excess USB ports available. Since the USB can handle communication rates of at least 1 Mbps and it also works well for bench testing with a laptop, it was decided to use USB to interface with the computer. USB uses its own protocol to transmit data, with specific synchronization sequences, packet sizes, and end-of-packet indicators. As mentioned above, these protocol specifics do not matter, since they will be passed through the optical transmitter like any other data. What is important is how binary zeros and ones are indicated. USB uses differential voltages, sent over a twisted pair cable, to communicate. A “1” is received when the D+ line is 200mV greater than the D- line, and a “0” is received when the D+ line is 200 mV less than the D- line (30). USB uses a specific communication protocol. Since this is not how TTL logic works, a USB-TTL converter was needed.

The FT232R USB-TTL level serial converter cable does just that. It uses a FT232RQ chip, housed within a USB connector, to turn USB data into asynchronous serial data at TTL levels. In RS232 serial communication, a binary “1” is represented by a negative voltage and a binary “0” is represented by a positive voltage. This means that when the serial data gets shifted to TTL levels in the cable, a logical “0” is +5 volts and a logical “1” is zero volts. This reversal doesn’t matter to the transmitter, but in an effort to conserve system battery energy and prevent the LED from overheating, a 74HC14 inverting Schmitt trigger was placed between the cable and the MOSFET driver to reverse the values. This means that a logical “0” is again represented



Figure 14 TTL232R USB-TTL Level Serial Converter Cable from FDTI

by 0 volts and a logical “1” is represented by +5 volts (see Figure 15 for Schmitt inverter schematic symbol and truth table). Without the inverter, the logical “0” of a dead line (no communication) would be represented by +5 volts, which would turn the MOSFET “on” and the LEDs would be constantly illuminated while idle, draining the battery!

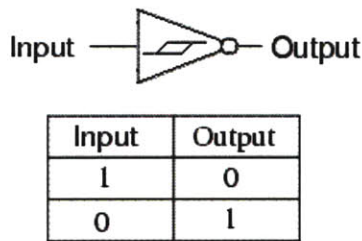


Figure 15 Schmitt inverter and truth table (31)

3.1.4 Testing the Transmitter System

Figure 16 shows the assembled transmitter system. Data is sent from the computer through a USB-TTL converter cable to the LED driver (which consists of the power MOSFET and MOSFET driver) that switches the Titan series LED lighting system on and off.



Figure 16 Transmitter system

Once this was assembled, the LED driver circuit (see Figure 10) was constructed on a breadboard and the transmitter system was tested to assess performance. Figure 17 shows the test setup. The first picture (a) shows the LED lamp mounted on a metal bar so as to overhang the ledge. The bread board - close up in picture (b) – is attached to the top of the metal bar and two power supplies are used to provide +12V (for the MOSEFT driver) and +24V (to power the LEDs). What can't be seen in either picture is the signal generator that created the square wave input signal to the circuit (taking the place of the computer and USB-TTL converter cable in

initial testing). Since the USB-TTL converter cable was not used in initial testing, the 74HC14 inverter was unnecessary and therefore not hooked up to the LED driver circuit.

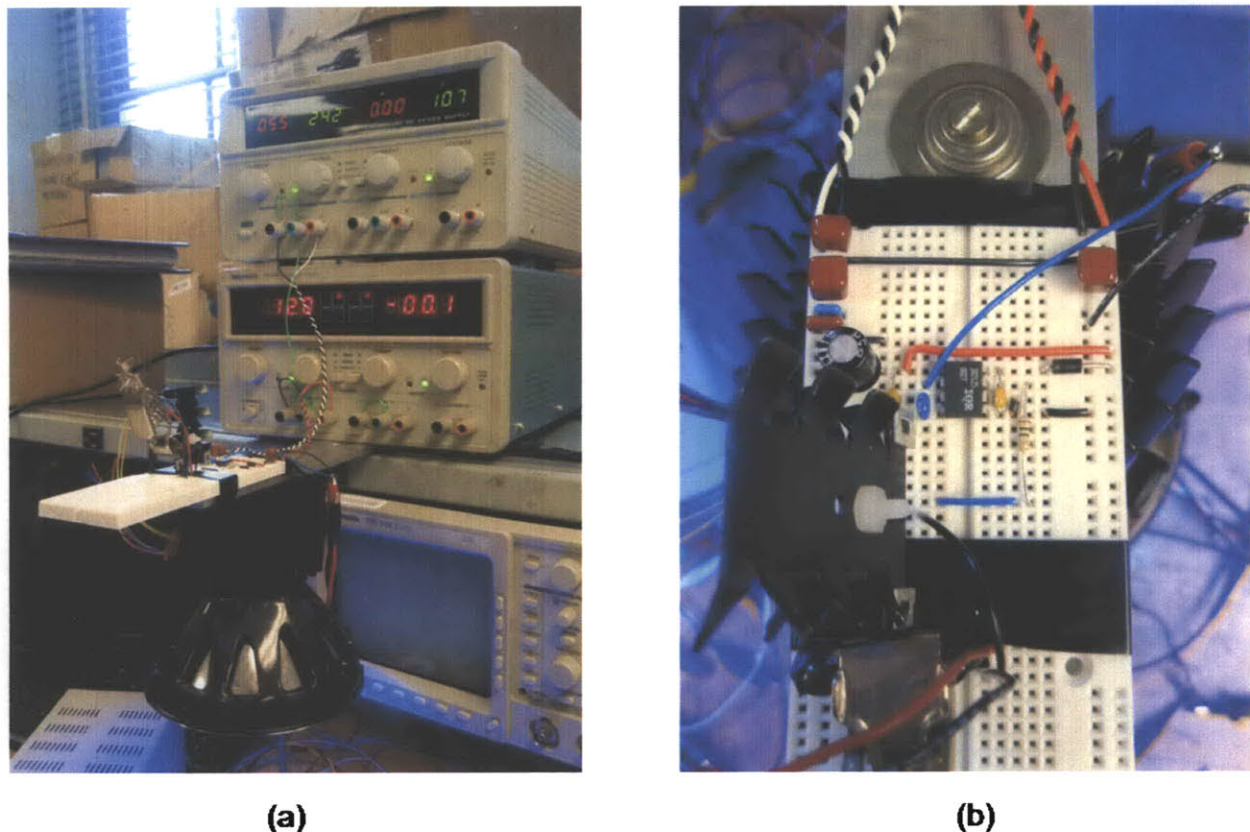


Figure 17 Testing the transmitter design.

In order to understand the transmitter's ability to communicate at various data rates, the signal generator drove the transmitter with various speed square waves while the input signal (from the signal generator), the gate voltage and drain voltage were monitored on an oscilloscope (also not pictured). In the following oscilloscope screen shots: trace 1 (orange) is the signal generator input signal to the MOSFET driver; trace 2 (blue) is the voltage at the MOSFET gate; trace 3 (purple) is the drain of the MOSFET, when the MOSFET is “off” the drain voltage is high, when the MOSEFT is “on”, current is allowed to flow through the MOSFET, connecting the drain pin to the source pin, which is tied to ground; and trace 4 (green) is not relevant to the discussion. See Figure 18 for the oscilloscope probe placements as they correspond to the oscilloscope screen print trace number and color.

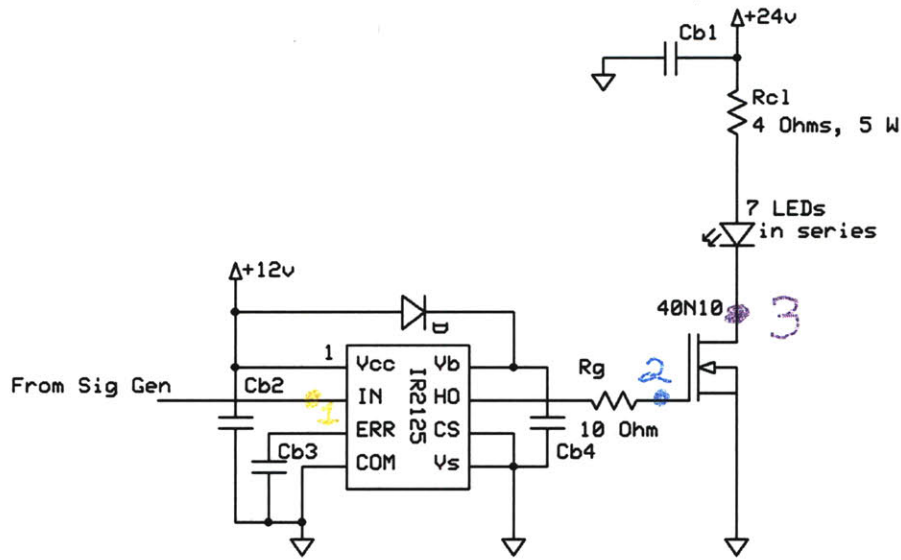


Figure 18 Oscilloscope test probe locations for the subsequent screen grabs.

When the system was first tested, there were only a couple of basic bypass caps in the circuit and the current-limiting resistor was a single 4 ohm, wire wound resistor that was found in the lab. Between the parasitic inductance and capacitance in the resistor and the parasitic capacitance inherent in the LEDs, an LC circuit was unintentionally created. As a result, when the MOSFET switched states, turning on and off 24 watts of power, the system experienced significant ringing.

This can be seen in Figure 19. In this instance only, trace 4 (green) is the ground rail and the 2125 MOSFET driver is being used. In this test, the signal generator is driving the transmitter at 1 MHz. You can see that the 2125 MOSFET driver takes a significant amount of time to ramp up the gate voltage (as discussed in section 3.1.2). Additionally, you can see the incredible amount of ringing in the system, especially when the MOSFET turns “off” and the drain voltage spikes to over 35 volts! This ringing affects the entire system, not just the 24 V power rail, as can be expressly noted by looking at the 8.2 peak-peak voltage seen on the ground rail in trace 4.

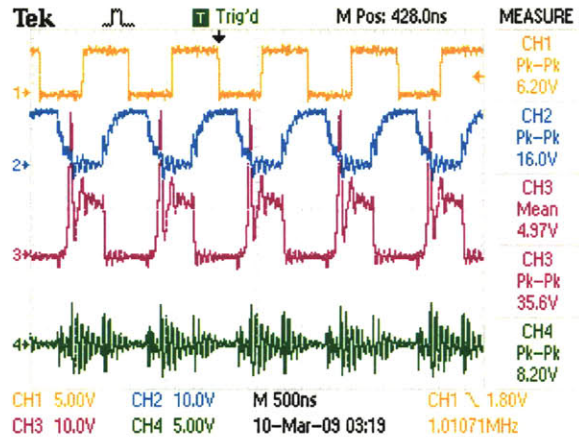


Figure 19 Initial transmitter tests

In order to reduce this ringing a couple steps were taken. The first was to switch out the single 4 ohm wire-wound resistor for four 1 ohm ceramic resistors in series. This change from using wire-wound to ceramic resistors drastically decreased the parasitic inductance in the resistor, since current was no longer flowing through a coiled wire. Additionally, switching from a single resistor to four smaller resistors reduced the parasitic capacitance. This happens because though resistors add when placed in series, capacitors in series result in a total capacitance that is less than any single capacitor in series (see Equation 1).

$$\frac{1}{C_T} = \frac{1}{C_1} + \frac{1}{C_2} + \dots + \frac{1}{C_n}$$

Equation 1 Capacitors in Series

Finally, more appropriate and more total by-pass capacitors were used between the 24 volt supply and ground. Large value electrolytic by-pass caps ($1000\mu\text{F}$) were replaced with low ESR capacitors and $47\mu\text{F}$ tantalum by-pass capacitors were added. Additionally, many small (0.01 - $0.1\mu\text{F}$) ceramic by-pass capacitors were added. These changes, along with upgrading the MOSEFT driver, resulted in a much cleaner signal overall.

Figure 20 shows the results of testing after making these changes. Like Figure 19, Trace 1 is the input signal, trace 2 is the gate voltage, and trace 3 is the drain voltage. You can see that the ringing has been significantly reduced and that the peak voltage experienced by the MOSFET drain is only 25 volts, instead of the previous 35 volts.

The importance of using ceramic resistors over wire-wound ones in this situation can be seen in Figure 21.

The first oscilloscope screen shot (a) shows the circuit with four, 1 ohm wire-wound resistors being used at the current-limiting resistors. The second screen shot (b) shows the exact same circuit, but the four wire-wound resistors have been replaced with four 1 ohm ceramic resistors. The peak drain ringing voltage has been reduced by 20% when using the ceramic resistors and the general ringing has also been reduced.

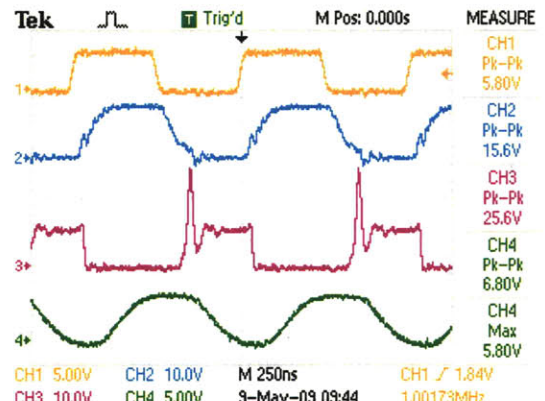


Figure 20 Improved transmitter testing.

The peak drain ringing voltage has been reduced by 20% when using the ceramic resistors and the general ringing has also been reduced.

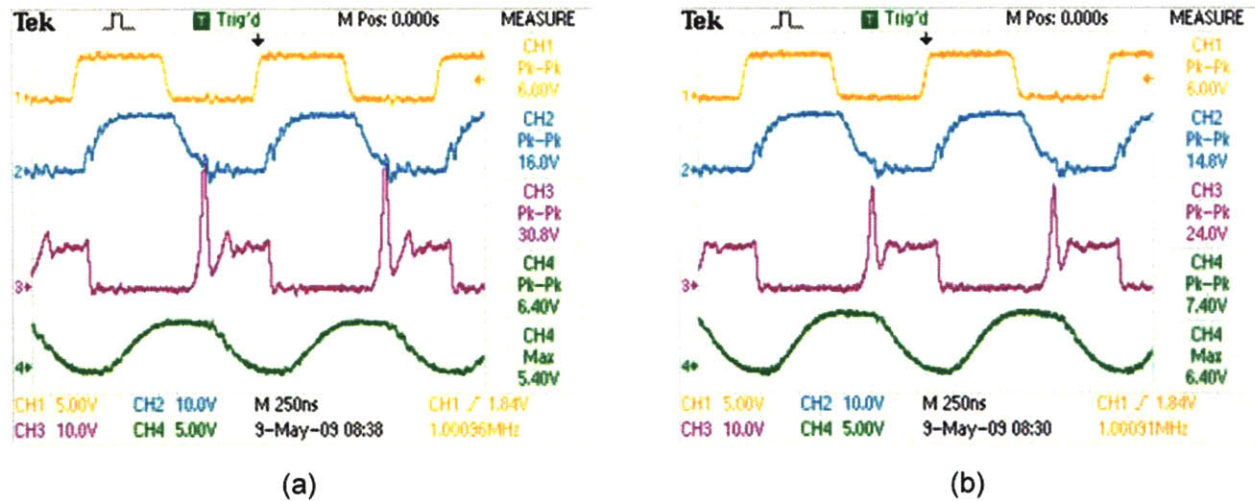


Figure 21 Wire-wound (a) vs. Ceramic (b) current-limiting resistors

3.1.5 Finalizing the Transmitter System

Once the tests had been conducted, a finalized circuit layout was determined (see breadboard with multiple small capacitors and four 1 ohm ceramic capacitors in Figure 22).

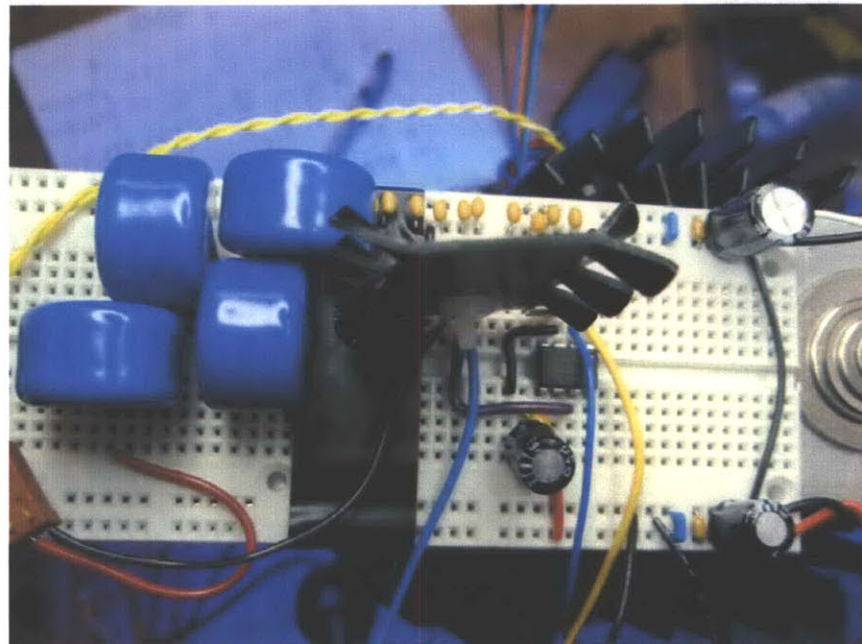


Figure 22 Final breadboard testing, the blue disks are 1 ohm ceramic resistors.

inductance inherent in breadboards and long wire leads. It was decided that the circuit board should fit the PC104 footprint so that it would easily be integrated with other systems. Additionally, prototyping space was included since it is well known that something is always forgotten. In this case, it turned out to be a great idea! As mentioned previously, initial tests did not utilize the USB-TTL cable, so the inverted voltage issue was not identified. Accordingly, no inverter was included in the original schematic or PCB layout. Thankfully, the prototyping space made it possible to retrofit the board with an inverter. Figure 24 shows the mechanical layout of the printed circuit board (PCB) and Figure 25 shows the actual board populated with components and altered to include the inverter.

Unfortunately, modifying the board to include the inverter added more stray capacitance and therefore made the signals have more ringing and noise. This can be seen in Figure 23, where trace 1 (orange) is the input signal to the board (3 Mbps), trace 2 (blue) is the output of the inverter, trace 3 (purple) is the gate of the MOSFET, and trace 4 (green) is the drain of the MOSFET.

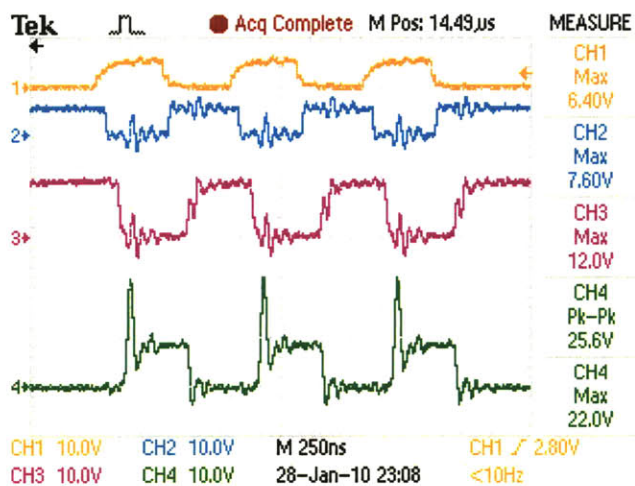


Figure 23 Final transmitter testing with inverter added to the PCB

In future revisions, including the inverter as a surface mount component will greatly improve the signal. Additionally, it would be good to include test points to easily monitor the system, a key learning that was implemented with great success in the receiver printed circuit board.

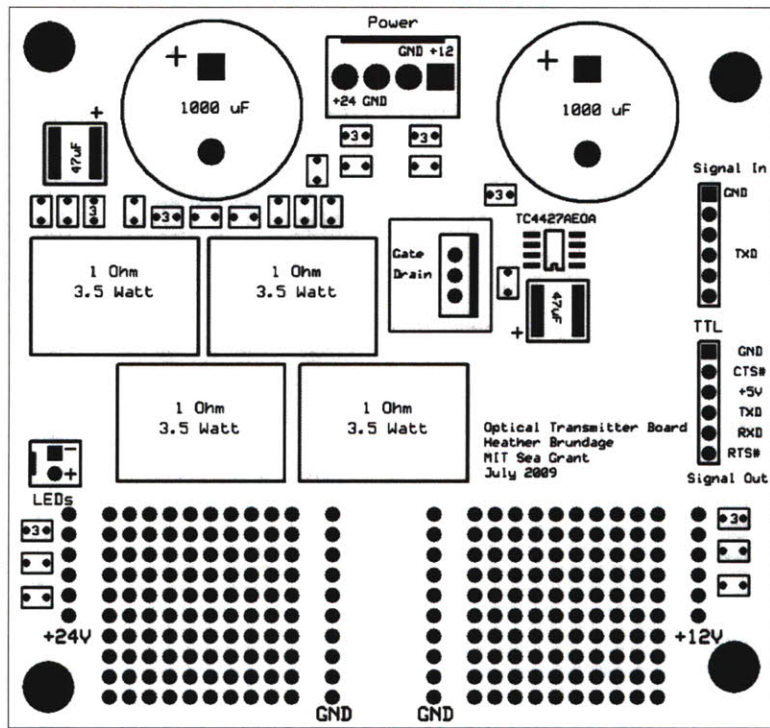


Figure 24 Transmitter PCB mechanical layout

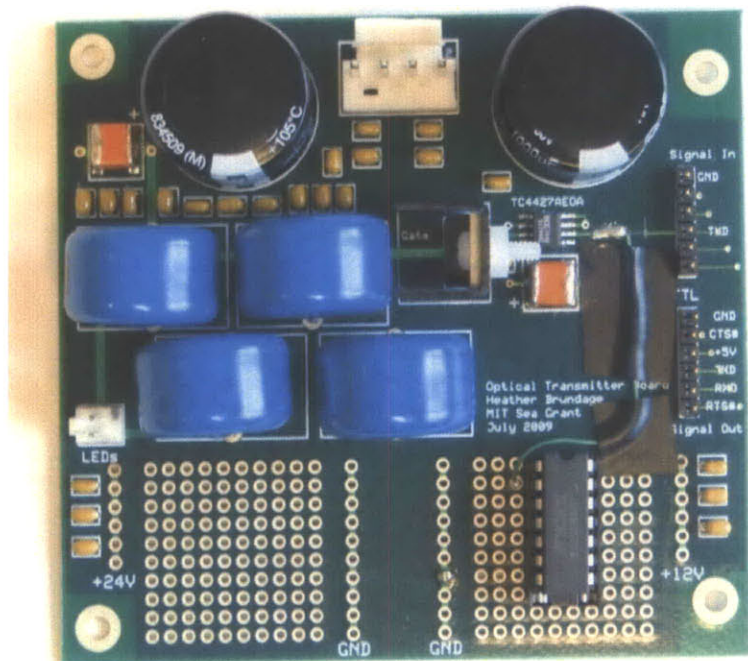


Figure 25 Populated transmitter printed circuit board

3.2 Optical Receiver

The optical receiver system detects the optical signal and transforms it into an electrical signal. It consists of a photon detector, which converts an optical signal into an electrical current, as well as additional electronics to convert the photon detector's electrical signal into TTL voltage levels. Figure 26 shows this the system-level receiver design.

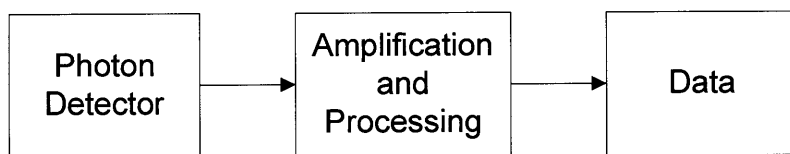


Figure 26 Receiver system diagram

Like the optical transmitter, the optical component of the receiver (in this case, the photon detector) determines the design of the rest of the system, which solely exists to condition the optical components output into a usable electrical form. Accordingly, the photon detector must be selected before the rest of the receiver design can continue.

3.2.1 Photon Detector

There are many different types of opto-electrical devices that can be used as photodetectors. Ideally, a photodetector would be able to quickly respond to all incident photons sent by the transmitter without introducing additional noise. Additionally, it would be small, robust, cheap, and power efficient. Unfortunately, many of these qualities are mutually exclusive and trade-offs must be made. In our application, switching speed is the top priority for a photon detector, followed by light sensitivity. Of course, this is assuming that power and size constraints are met. In the following sections, I will discuss different possible photon detectors and their strengths and weakness as they relate to an optical communications receiver.

3.2.1.1 Photoresistors

Photoresistors (see symbol in Figure 27), also known as light dependent resistors or cadmium sulfide (CdS) cells, are a type of photoconductor, meaning that their conductivity changes when exposed to electromagnetic

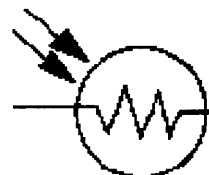


Figure 27
Photoresistor
symbol

radiation such as visible light(32). Photoresistors have a very high resistance, which can measure in the mega ohms (they are not conductive), when they are in the dark. When exposed to light, their resistance decreases linearly (over small regions) and may be as low as only a couple hundred ohms (19). Though they have very good light sensitivity, they respond very slowly. It typically takes over a millisecond for a photoresistor to fully respond to the presence of light. Additionally, it can take a couple of seconds for the photoresistor to return to its dark resistance after the light signal has ended. This is unacceptably slow for switching speeds of over 1 MHz.

3.2.1.2 Photothyristors

Photothyristors are another type of photodetector. They are just photo-activated thyristors, which are modified diodes. Like diodes, thyristors conduct current when their anode has a higher voltage than their cathode. But unlike diodes, thyristors have a third lead (the gate) that controls whether the thyristor starts conducting current. The gate must have a positive voltage and sufficient current before the thyristor will turn on (33). After the thyristor is activated, the gate does not affect the thyristor anymore. This means that once a photothyristor has been optically triggered, turning off the light will not turn off the thyristor – only turning off power to the circuit or making the cathode have a positive voltage compared to the anode will do that. For this reason, photothyristors are not ideal for optical communication purposes.

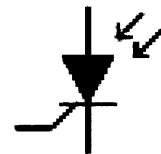


Figure 28
Photothyristor
symbol

3.2.1.3 Phototransistors

Phototransistors (see symbol in Figure 29) are like regular bipolar transistors or FETs, only their base (bipolar transistors) or gate (FETs) is exposed to light. When the photons hit the base or gate, either a current (bipolar transistors) or a voltage (FETs) is produced which starts to turn “on” the transistor (19). This means that when the phototransistor is in the dark, very little current flows through the transistor, but in the presence of light, the current or voltage signal produced by the light is amplified by the

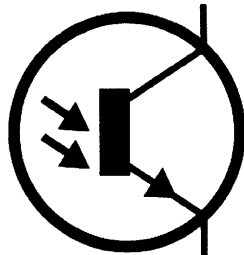


Figure 29
Phototransistor
symbol

transistor's current gain as the transistor turns on and allows current to flow from the collector to the emitter. This internal gain (from one hundred to several thousand) makes phototransistors incredibly sensitive to any light signal (34). Unfortunately, they are only moderately fast (250 KHz) even though they are relatively robust with regards to noise (35).

3.2.1.4 Photomultipliers

Photomultiplier tubes (PMTs) are a type of vacuum tube that is very light sensitive (see Figure 30). Incident light produces electrons, which are accelerated and multiplied by dynode plates. The current can be multiplied over a million times after going through multiple dynode stages (34). Photomultiplier tubes are great for detecting low light level signals, as they are able to detect even single photons. Because of their high sensitivity, they are easily affected by ambient light. In order to produce such high gains, photomultipliers are large and need high voltage levels (thousands of volts) (36). They are fragile, easily affected by magnetic fields, and expensive. Even though they can have a response time of less than a nanosecond (37), their size, power consumption and fragility make them a poor choice for underwater optical communication.



Figure 30 Picture of a photomultiplier (20)

3.2.1.5 *p-n* Photodiodes

Like the previous photon detectors, photodiodes convert light energy into electrical current. When incident light hits the photodiode, it turns the photodiode into a current source that pumps current from the cathode to the anode (19).



Photodiodes consist of *n*- and *p*-type semiconductors sandwiched together. The *p*-type has a surplus of holes and the *n*-type has excess electrons. Where the two types meet, the depletion region, holes and electrons recombine in order to equalize the number of free carriers in the semiconductor. This produces a positive net charge in the *n*-type material and a negative charge

in the p-type material, due to the reduction of free electrons and holes, respectively. This charge build up prevents more (positive) holes crossing the depletion region to bond with free electrons in the n-type material, and vice versa (38).

When a photon passes through the diode it can excite an electron, creating an electron-hole pair. If this happens close enough to the depletion region, the inherent electric field will push holes towards the anode (*p* side) and electrons towards the cathode (*n* side). This separation of charges leads to a voltage potential across the pn junction. This potential produces a photocurrent, as electrons flow from the electron-abundant cathode towards the hole-abundant anode (19).

The electric field resulting from the depletion region is often augmented by an external electric field that reverse biases the diode. A stronger electric field produces a larger depletion region, which in turn increases the quantum efficiency (the devices' sensitivity to light, see Equation 2) by giving photons more time to (and therefore a greater chance of) exciting electrons. A larger depletion region reduces the junction capacitance (which helps increase bandwidth), but also increases the amount of time it takes electron-hole pairs to transit across and out of the depletion region, decreasing bandwidth. This trade-off between quantum efficiency (which continues to increase with larger depletion regions) and bandwidth (which initially increases, then decreases as the depletion region increases) is inherent in all photodiodes (38).

$$\eta = \frac{\# \text{ of photocarries produced}}{\# \text{ of incident photons}}$$

Equation 2 Equation for Quantum Efficiency, η , of a photodetector

Since each photon can only excite one electron at most, photodiodes do not have any internal gain, but they are incredibly linear. Additionally, since photons can go through a diode without exciting any electrons, photodiodes do not have the sensitivity (quantum efficiency) of photomultiplier tubes that can detect single photons. Photodiodes can have rise times as short as 10 picoseconds and are relatively robust to noise (34). They are small, robust, and affordable.

3.2.1.6 Avalanche Photodiode

Avalanche photodiodes are similar to p-n photodiodes, except that they can generate multiple electron-hole pairs as a result of absorbing a single photon (38). This multiplication effect is due to a strong electric field across the photodiode which gives photon-generated electrons enough energy to create secondary electron-hole pairs, which in turn can create more electron-hole pairs in avalanche multiplication (22). The internal gain, which can be on the order of 10^2 to 10^4 , gives the avalanche photodiodes much more sensitivity, but also introduces more noise into the signal, especially in the presence of ambient light (20). Avalanche photodiodes are non-linear, since their multiplication is non-linearly dependant on supply voltage and temperature. Because of their sensitivity to these factors, special circuitry is needed – adding complexity and cost while reducing reliability. They also require large supply voltages, ranging from 30-300 volts (20).

3.2.1.7 Photon Detector Selection

As can be seen in the sections above and Table 4 below, there are many factors to take into account when selecting a photon detector. Though photomultipliers are very sensitive and fast, they are large and power hungry. Phototransistors and photoresistors work great as light-activated switches, but are not fast enough for communications. Fortunately, photodiodes fit the requirements necessary for wireless underwater optical communications.

	Photoresistors	Phototransistors	p-n Photodiodes	Avalanche Photodiodes	Photomultipliers
Speed	Slow $<1\text{ Hz}$	Moderate $<250\text{ KHz}$	Fast <i>Tens of MHz to tens of GHz</i>	Fast <i>Hundreds of MHz to tens of GHz</i>	Fastest $>1\text{ GHz}$
Size	Small	Small	Small	Small	Large
Gain	Little	100-1500	Unity	100-10,000	$>1\text{ million}$
Linearity	Over small regions	Good	Excellent	Not Linear	Good
Ambient Noise Performance	Very good	Excellent	Very Good	Fair	Poor

Table 4 Comparison of photodetectors (34)(20)(19)(36)

Though avalanche photodiodes are potentially faster and have the added advantage of a high internal gain, a p-n photodiodes was selected as the photodetector for the optical receiver. This

was because of the high bias voltage required to operate avalanche photodiodes, as well as their sensitivity to noise and their higher complexity of control circuitry.

In searching for the exact photodiode to use, qualities such as quantum efficiency, bandwidth and sensitivity to 470 nm light were considered. The last criterion was a challenge to find, since the material that most photodiodes are made out of (silicon) is much more receptive to light in the red or infrared spectrum. Figure 31 shows the spectral response of various types of photodiodes made by Pacific Silicon Sensor. You can see that most of the photodiodes have peak sensitivity in the 800-1000 nm range and have very limited sensitivity in the 400-500 nm range. Only one series, 6B which is blue enhanced, has significant sensitivity to blue light.

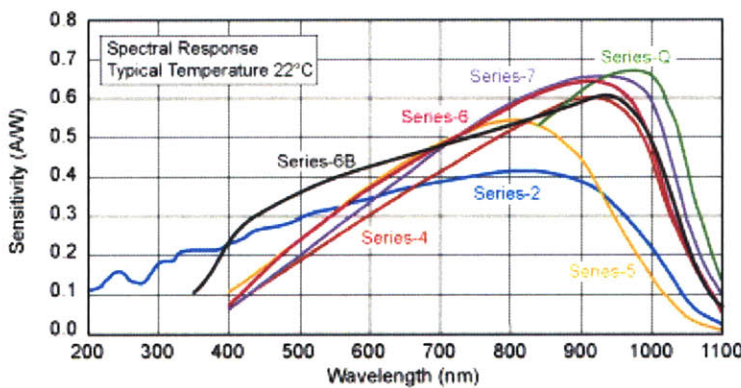


Figure 31 Spectral response of various photodiodes (39)

There are many other manufacturers of photodiodes, but few produce blue-enhanced photodiodes, and of those photodiodes, many have a very slow response time as a side effect of the blue light sensitivity enhancement. Pacific Silicon Sensor offered photodiodes with >70% quantum efficiency at 410 nm, low dark current (which contributes to noise), and fast rise times (under 50 ns). Part number PC10-6B (see Figure 32) was selected as a good trade-off between active area (10mm^2 - bigger area means more sensitivity) and rise time (20 ns – faster rise time means better bandwidth). A 24 V reverse bias across the photodiode was used to increase the bandwidth and quantum efficiency, as discussed in section 3.2.1.5, since it was the largest voltage easily available on the test platform that was also within the allowable range for the photodiode.

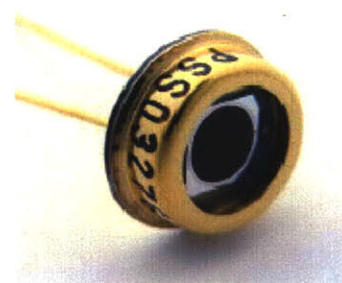


Figure 32 PC10-6B

3.2.2 Signal Processing

Once a photodiode was selected, the next step was to design the required electronic circuitry to condition and process the photodiodes current signal. Figure 33 shows the main components needed. First, the photodiodes current signal needs to be transformed into a voltage signal, which is then amplified and finally made compatible with TTL voltage levels.

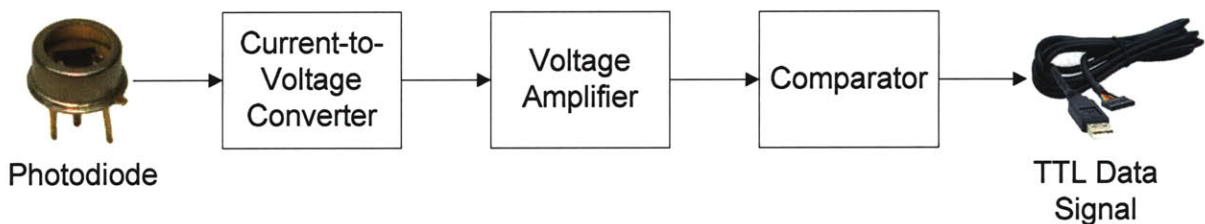


Figure 33 Receiver electrical system diagram

3.2.2.1 Current-to-Voltage Converter

As discussed in section 3.2.1.5, photodiodes act as current sources when exposed to light. Though this current signal is very linear, most electrical devices work based on changes in voltage levels, as opposed to changes in current levels. For this reason, the current signal coming from the photodiode must first be converted to a voltage signal. There are a couple different ways of achieving this transformation.

3.2.2.1.1 Theory

The most basic current-to-voltage converter uses Ohm's law ($V = I \cdot R$). A resistor is placed across the current source, causing a voltage drop across the resistor (see Figure 34). This voltage drop is proportional to the current, scaled by the resistor value, thereby successfully converting a current signal into a proportional voltage signal.

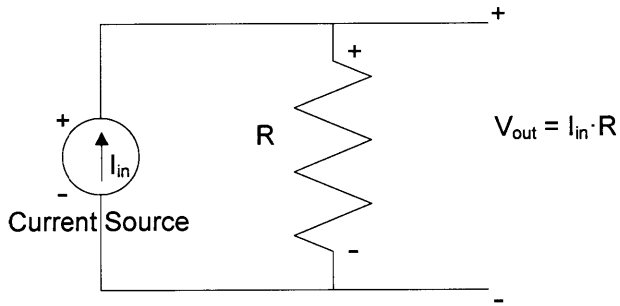


Figure 34 Basic passive current-to-voltage converter

Though this arrangement works in theory, it is not as practical in actual implementation. This is because this passive current-to-voltage converter assumes that the load (whatever is hooked up to V_{out}) has infinite resistance. Though components with very high resistance are possible, an infinite resistance is physically impossible. Instead, every load will have a finite resistance which will cause a portion of the current to be diverted to flow through the load. This reduces the current that flows through the resistor, thereby reducing the voltage drop across the resistor and the corresponding V_{out} . So by placing a component on the circuit to monitor it, the circuit characteristics change! Additional problems result if the resistance is too high, as the leakage current from the photodiode could saturate the photodiode, preventing a modulated signal from being detected. Saturation results when the reversed biased voltage across the photodiode is similar to the voltage drop across the resistor (40). Too high of a resistor value also causes the response time to be slow, due to the parasitic capacitance inherent in the photodiode (41). As you can see in Equation 3, the time constant is proportional to the resistor value times the capacitance in the photodiode. That means that the higher the resistor value, the higher the gain of the circuit, but the slower the response.

$$t = R \cdot C_p$$

Equation 3 Time constant

An improved current-to-voltage converter is called a transimpedance amplifier, and it consists of a resistor (and sometimes a capacitor in parallel) across an operational amplifier (op-amp) (see Figure 35). This connects the photodiode to a virtual ground, removing the parasitic capacitance of the photodiode from the equation, allowing for much larger gains at much faster response times.

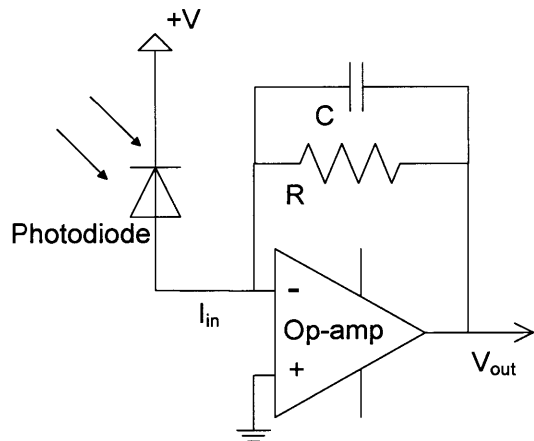


Figure 35 Transimpedance Amplifier

The value of the resistor, R , determines the gain of the transimpedance amplifier as shown in Equation 4. The feedback capacitor, C , is used to stabilize the circuit and reduce overshoot. Though there are some equations to help determine the ideal value of C , the precise value will need to be tuned experimentally to account for the specifics of each layout.

$$V_{out} = I_{in} \cdot R$$

Equation 4 Transimpedance amplifier output voltage

3.2.2.1.2 Design

When selecting components for the transimpedance amplifier, high speed and high gain were important. Texas Instruments' THS4631 op amp was chosen because it had a very high gain bandwidth product of 210 MHz and could run off the +12/-12 voltage rails (42). It was wired as in Figure 35, without the feedback capacitor initially. A feedback resistor value of 33K was chosen as a good compromise between high gain and high bandwidth. It also produced a clean signal. If the feedback resistor is too low, the gain is very small and the system can have too much ringing and noise, whereas if the feedback resistor is chosen to be too large, the gain is too high, saturating the signal and reducing the bandwidth.

This can be seen in Figure 36, where trace one (orange) is the signal driving the transmitter and trace two (blue) is the output of the transimpedance amplifier. You can see that in (a), where the feedback resistor is only 2.2K ohms, the gain is very low – the output voltage is only about -840mV. Additionally, the relationship between the low resistance and the high parasitic capacitance in the circuit (there is no additional feedback capacitor in this circuit, since that would only make it worse) means there is a lot of ringing. In (c), the feedback resistor is 330K ohms, producing such a large gain that the op amp is constantly saturated – it gives the maximum output voltage of -10 V. Figure (b) results in the cleanest signal (not perfect, as there is no feedback capacitor to reduce the overshoot) when using a feedback resistor of 33K ohms.

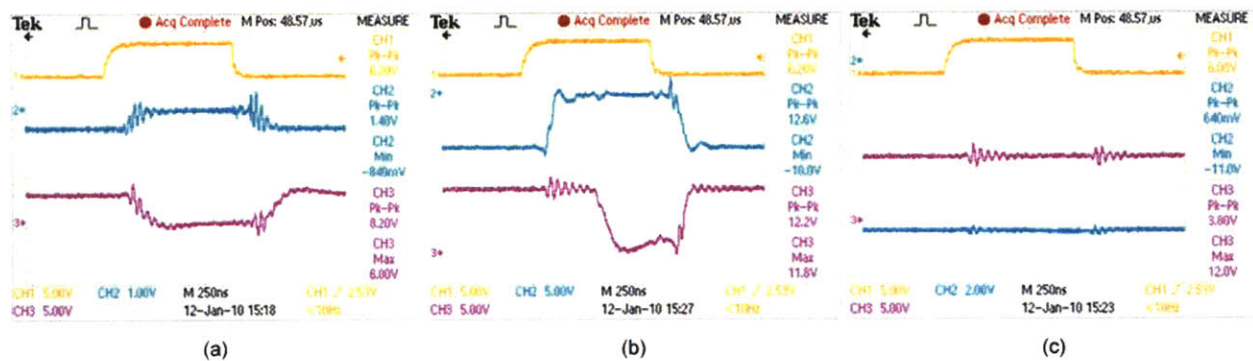


Figure 36 Transimpedance amplifier feedback resistor testing

(a) $R_f = 2.2\text{K}\Omega$ (b) $R_f = 33 \text{ K}\Omega$ (c) $R_f = 330\text{K}\Omega$

Once the op amp and feedback resistor were determined, testing was done to determine the best C_f for the circuit. If C_f is chosen to be too large, the time constant of the circuit will be too long and the switching speed reduced. An extreme case of this can be seen in Figure 37, where the traces are the same as before and the 33K ohm feedback resistor is being used, but this time an 8.2 μF feedback capacitor is in place across the transimpedance amplifier. You can see the slow ramp up indicative of a long time constant due to the relationship between the feedback resistor and capacitor.

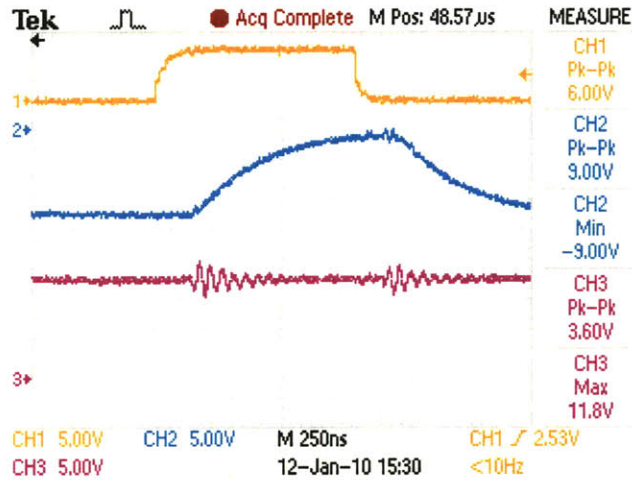


Figure 37 Output of transimpedance amplifier when C_f is too large.

Figure 38 shows fine tuning the feedback capacitor value. In (a), the capacitor value is too small so there is overshoot and ringing. In (c), the capacitor value is too high, so there is a slight ramp up. In (b), the capacitor value is just right, minimizing ringing and over-shoot, without increasing the time constant too much. This testing was done on a breadboard, which has a lot of parasitic capacitance. Once the circuit was moved to a printed circuit board, the feedback capacitor value was lower, since there is less stray capacitance in the PCB.

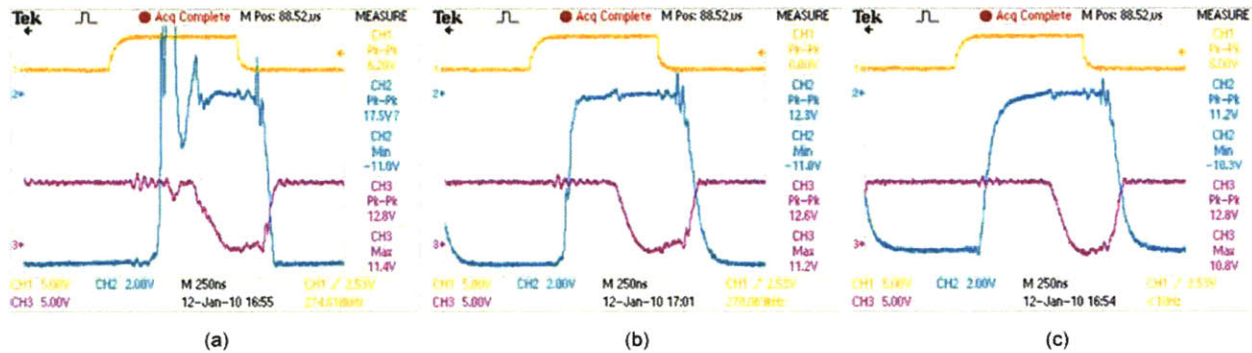


Figure 38 Tuning C_f (a) C_f too small (b) C_f just right (c) C_f too large

3.2.2.2 Voltage Amplifier

The next step in the signal processing is to add an inverting voltage amplifier. This changes the signal from a negative voltage to a positive voltage and amplifies it so that even very small signals, received when the transmitter is far away from the receiver, can be detected. A typical inverting amplifier is shown in Figure 39. Equation 5 shows how the ratio of the resistor values sets the gain for the circuit.

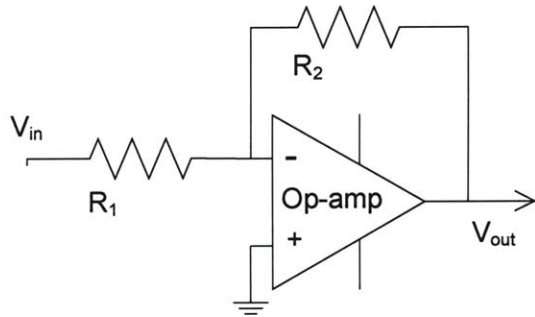
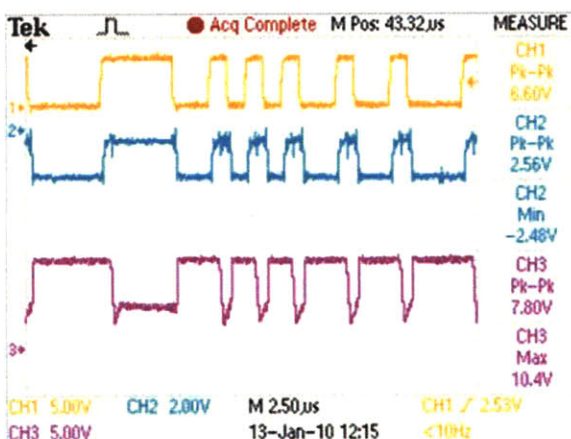


Figure 39 Inverting amplifier

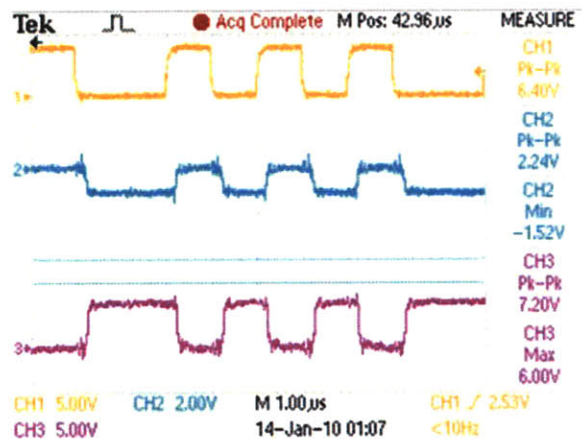
$$Gain = - \frac{R_2}{R_1}$$

Equation 5 Inverting amplifier gain equation

Similar to selecting the transimpedance amplifier component, the voltage amplifier requires an op-amp that is capable of high gains at high speeds. The response time of the op-amp must also be taken into account. Figure 40 shows the significance of selecting the correct component.



(a)



(b)

Figure 40 Comparing two different voltage amplifiers (a) LM318 (b) LM7171

In the figure, trace one (orange) is again the input signal to the transmitter. Trace two (blue) is the output of the transimpedance amplifier and trace three (purple) is the output of the inverting voltage amplifier. Picture (a) shows the results when a slower op amp is used, the LM318. It has a 200 ns response time which is too slow for a 1 MHz system! You can see how the delayed response results in shortened “0” pulses. Picture (b) shows the circuit when the LM318 was replaced by the much faster LM7171, which has a response time of 42 ns (43). The LM7171 is much better suited to this high speed application.

The resistor values were chosen to maximize gain without sacrificing speed. A gain of 7.7 was achieved with $R_1 = 1.3\text{K}$ ohms and $R_2 = 10\text{K}$ ohms. A filtering capacitor was placed across the op-amp, in parallel with R_2 to control the ringing by filtering high frequency noise. Equation 6 shows how the capacitor value was determined. Since the signal being sent would be a maximum of 3 MHz (limited by the capabilities of the USB-TTL converter cable), frequencies above 30 MHz could be filtered out. This results in using a capacitor with a value of 1 pF. You can see in Figure 40 (b) how these values produce a relatively clean signal with significant gain at 1 MHz.

$$f = \frac{1}{2 \cdot \pi \cdot R_2 \cdot C}$$

Equation 6 Equation to determine filtering capacitor value for the inverting voltage amplifier

3.2.2.3 Comparator

The final step is to convert the data signal into voltage levels that the TTL-USB cable (described in section 3.1.3) could accept – 0 and +5 volts. Since the previous step is an amplifier running off a +12 volt power rail, the signal coming from the amplifier can be anything between 0 and +11 volts, depending on the amplitude of the signal going into the amplifier from the transimpedance amplifier. If the transmitter is very close to the receiver in very clear water, that signal may saturate the receiver and produce a +11 volt signal at the output of the amplifier. If, on the other hand, the transmitter is further away from the receiver or the water quality is poor, the signal coming out of the amplifier may max out at a much lower voltage. Of course, if the signal is too weak, the receiver won’t register it at all!

In order to standardize the output of the receiver, a comparator is used to guarantee that the only outputs of the receiver are 0 and +5 volts. A comparator takes in two signals, compares them, and tells you which signal is larger. If the input signal is larger than the reference signal, then the comparator output goes high. Conversely, if the input voltage is lower than the reference voltage, the output goes low. You can see this in Figure 41 where the top trace is the input voltage, the bottom trace is the output voltage, and the horizontal line is the reference voltage. The high and low output voltage of the comparator is set by the circuit design, and in this case, a “high” output of +5 volts and a “low” output of 0 volts was desired.

A comparator is often built on an op-amp (just as the transimpedance amplifier and voltage amplifier are). The reference voltage is connected to the inverting input and the signal is connected to the non-inverting input (see Figure 42). The AD790 was selected as the comparator because it has a short delay time (45 ns), can operate off the already existing +12 voltage rail, and can handle input signals up to +12 volts. A potentiometer was used to create a voltage divider to supply the reference voltage. This allowed the reference voltage to be easily tuned during testing. A lower reference voltage means that any small signal could trigger the comparator, possibly making the circuit react to noise, but also allowing it to respond to very low input signals.

3.2.3 Receiver Testing

Bench testing on a breadboard was done to confirm the receiver system design before moving to a printed circuit board. Working on a breadboard is challenging when dealing with signals ≥ 1 MHz, since there is so much stray capacitance in the breadboard and in long wires. For this reason, the components were placed as close together as possible and wire runs were kept short and neat. Figure 43 (a) shows a close up of the receiver board without the comparator wired up and (b) shows the test set up, with the transmitter mounted above the receiver.

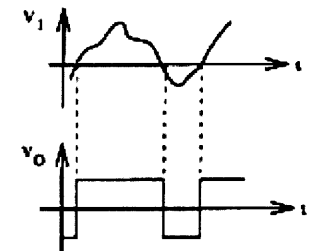


Figure 41 Comparator
input (top) vs output
(bottom)

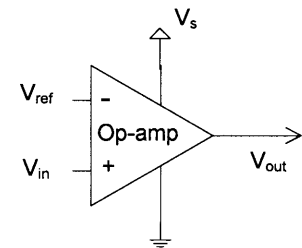
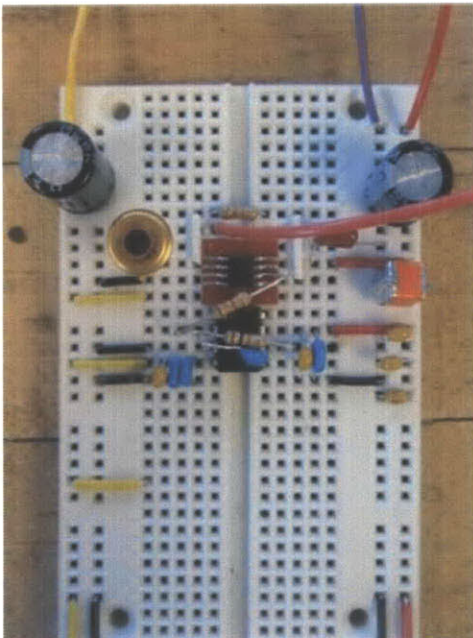


Figure 42 Op-Amp
Comparator Schematic



(a)



(b)

Figure 43 Receiver breadboard testing

Even though great care was taken to make the breadboard as robust as possible, the signals still contained significant noise, as can be seen in Figure 44, where trace 1 (orange) is the signal into the transmitter, trace 2 (blue) is the output of the transimpedance amplifier and trace 3 (purple) is the output of the voltage amplifier. A printed circuit board minimizes noise, so, since component selection was far enough along, a printed circuit board was constructed before further tests were performed. The design can be seen in Figure 45 and the constructed board can be seen in Figure 46.

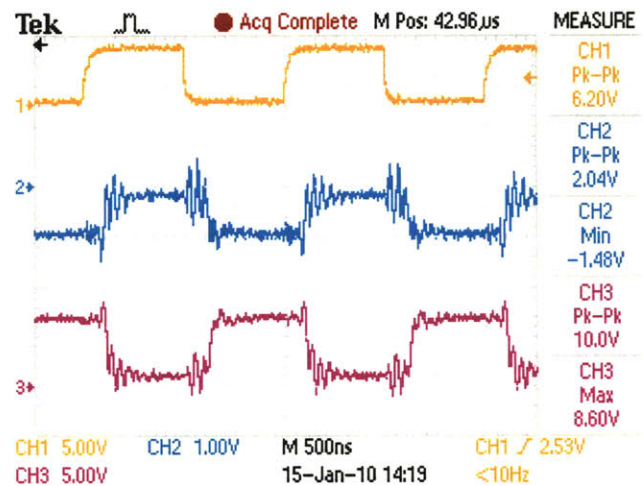


Figure 44 Ringing is present in the receiver circuit while testing on the breadboard.

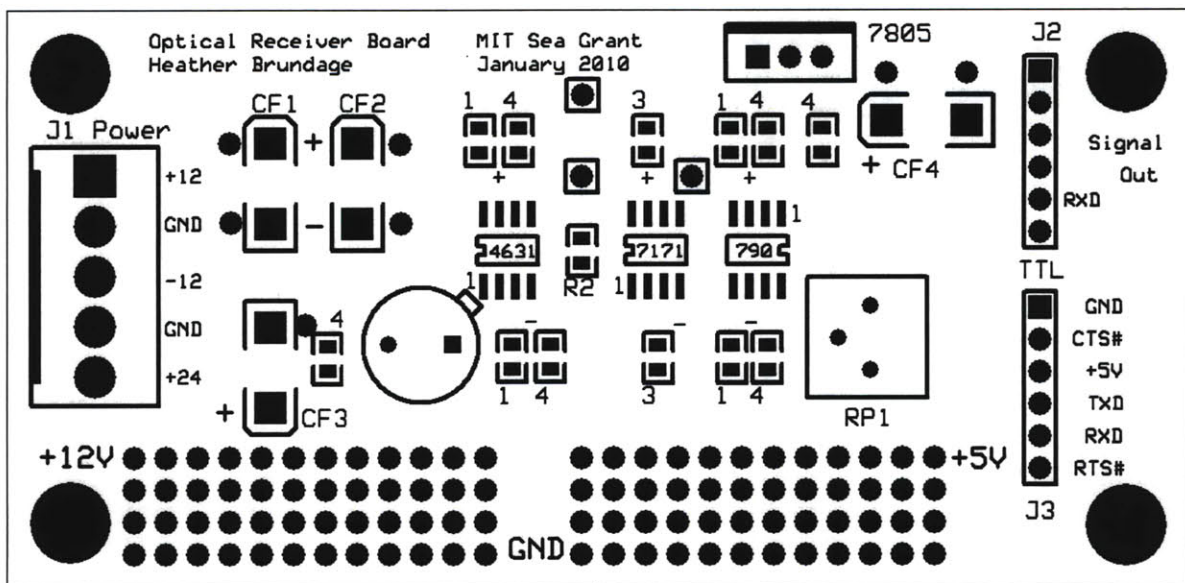


Figure 45 Receiver printed circuit board layout

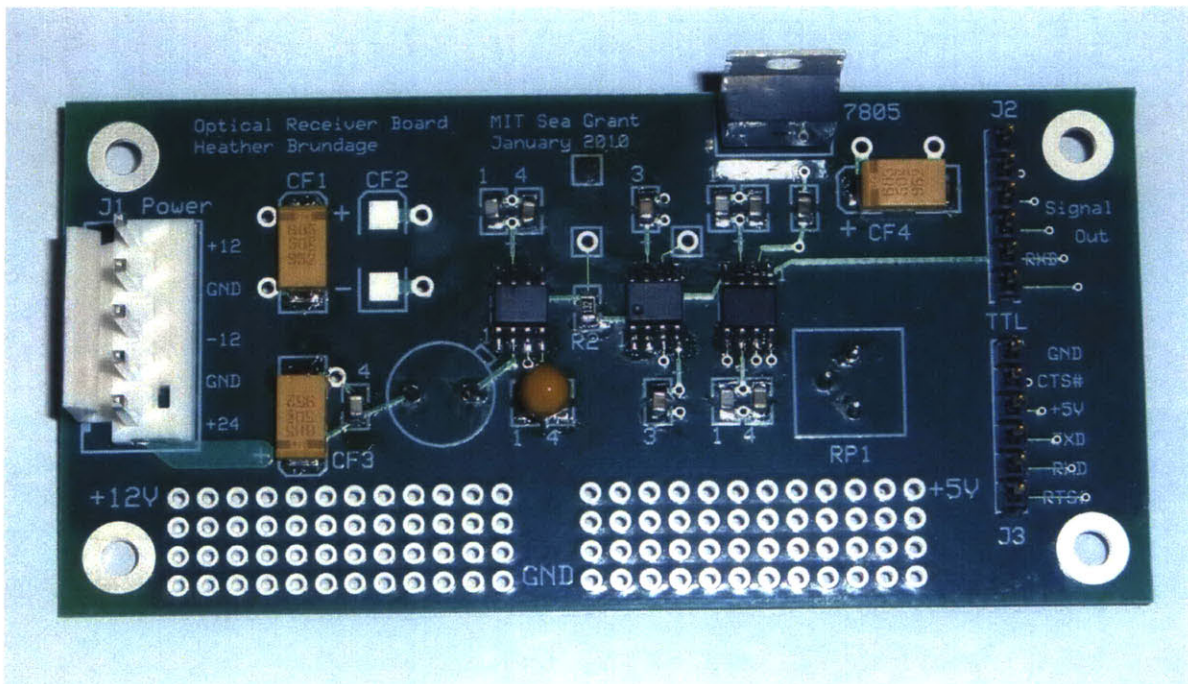


Figure 46 Back side of the receiver printed circuit board with components

Testing the receiver after it was constructed on the printed circuit board showed great improvement over the breadboard tests. The final schematic can be seen in the Appendix, but the signal traces can be seen in Figure 47. Trace 1 (orange) is the signal going into the transmitter, trace 2 (blue) is the output of the transimpedance amplifier, trace 3 (purple) is the output of the voltage amplifier and trace 4 (green) is the output of the comparator. You can see how crisp and clean the signal is, even at 3 Mbps.

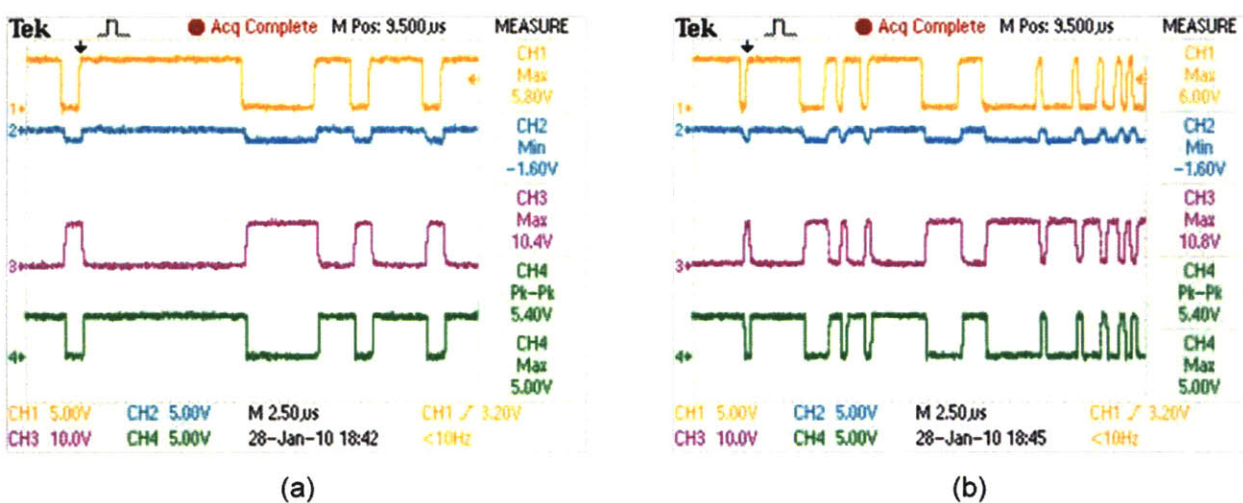


Figure 47 Receiver testing with the PCB (a) 1 Mbps (b) 3 Mbps

4 System Water Testing

Once the transmitter and receiver were both built and bench tested, it was time to test the system in water. Testing was performed in the MIT Tow Tank, a fresh water tank about a meter deep, 2.5 meters wide and 33 meters long.

4.1 Setup

The transmitter and receiver were mounted approximately 1 foot below the surface of the water, so that they could remain connected to power, signal, and oscilloscope probes during testing (see Figure 48). They faced each other and the transmitter could easily be moved a measurable distances away from the stationary receiver in order to test transmission over various distances.

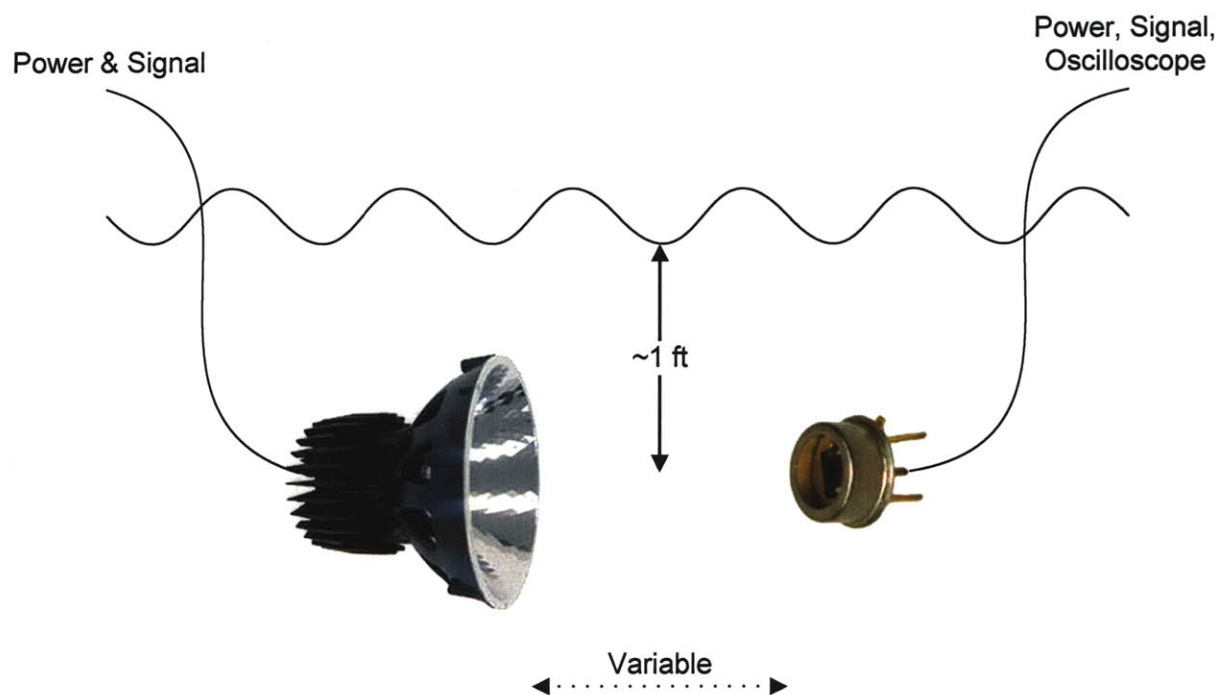


Figure 48 Water testing set up

4.1.1 Transmitter

Unfortunately, there was not time to create a waterproof housing with the appropriate penetrators for either the transmitter or receiver. Instead, an empty fish tank was ballasted to be mostly submerged. The LED module and transmitter PCB, mounted together on a metal plate, were placed in the fish tank, below the water level. The fish tank was connected to a moving platform above the tank so that it could easily be rolled closer and further away from the stationary receiver. The power supply and laptop computer required to power and send the data signal to the transmitter were placed on top of the platform so the whole system could easily be moved together (see Figure 49).

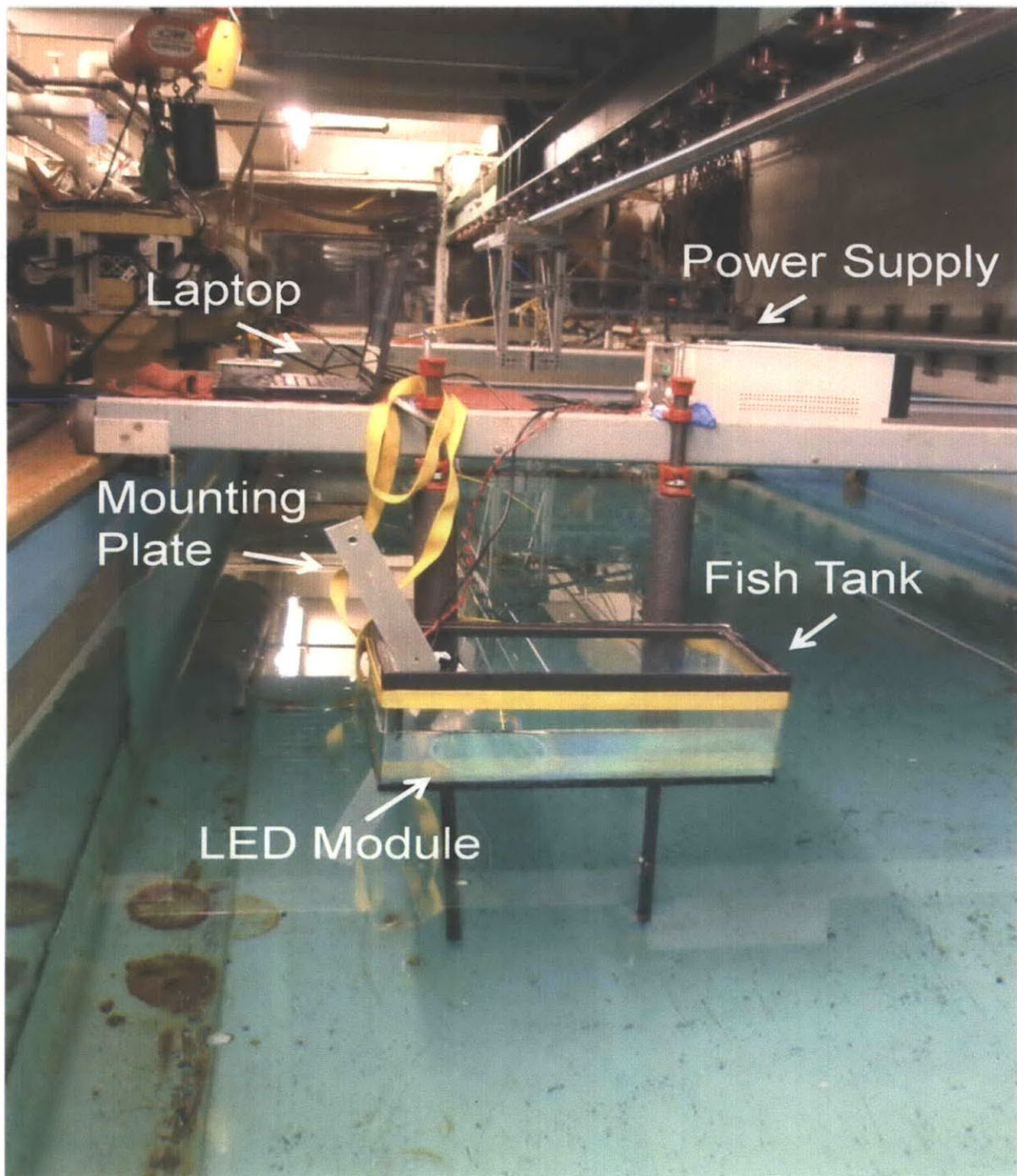


Figure 49 Transmitter water test set-up

4.1.2 Receiver

Like the transmitter, the receiver also had to be waterproofed, yet many more cables had to be connected. For this reason, the receiver was placed on a stationary mount. The circuit board was mounted on standoffs to a plastic chassis that helped protect the board, provided a secure means to mount the board below water, and acted as a cable guide. In order to protect the circuit from water, but still let the light reach the photodiode, the receiver system was placed in a plastic bag that was, like the fish tank, only partially submerged. Figure 50 (a) shows the circuit board mounted to the chassis with the cables connected. Figure 50 (b) shows the reverse side of the chassis – with the cutout for the photodiode – in the plastic bag.



(a)



(b)

Figure 50 Receiver water testing mount

Once the system was assembled, the chassis was bolted to a metal rod fixed above the test tank, as can be seen in Figure 51. Figure 52 shows the entire set-up of the receiver system. You can see that the power supplies, computer, oscilloscope and lab notebook were placed on the side of the tank since they did not have to move during testing.



Figure 51 Semi-submerged receiver mounted in the tank

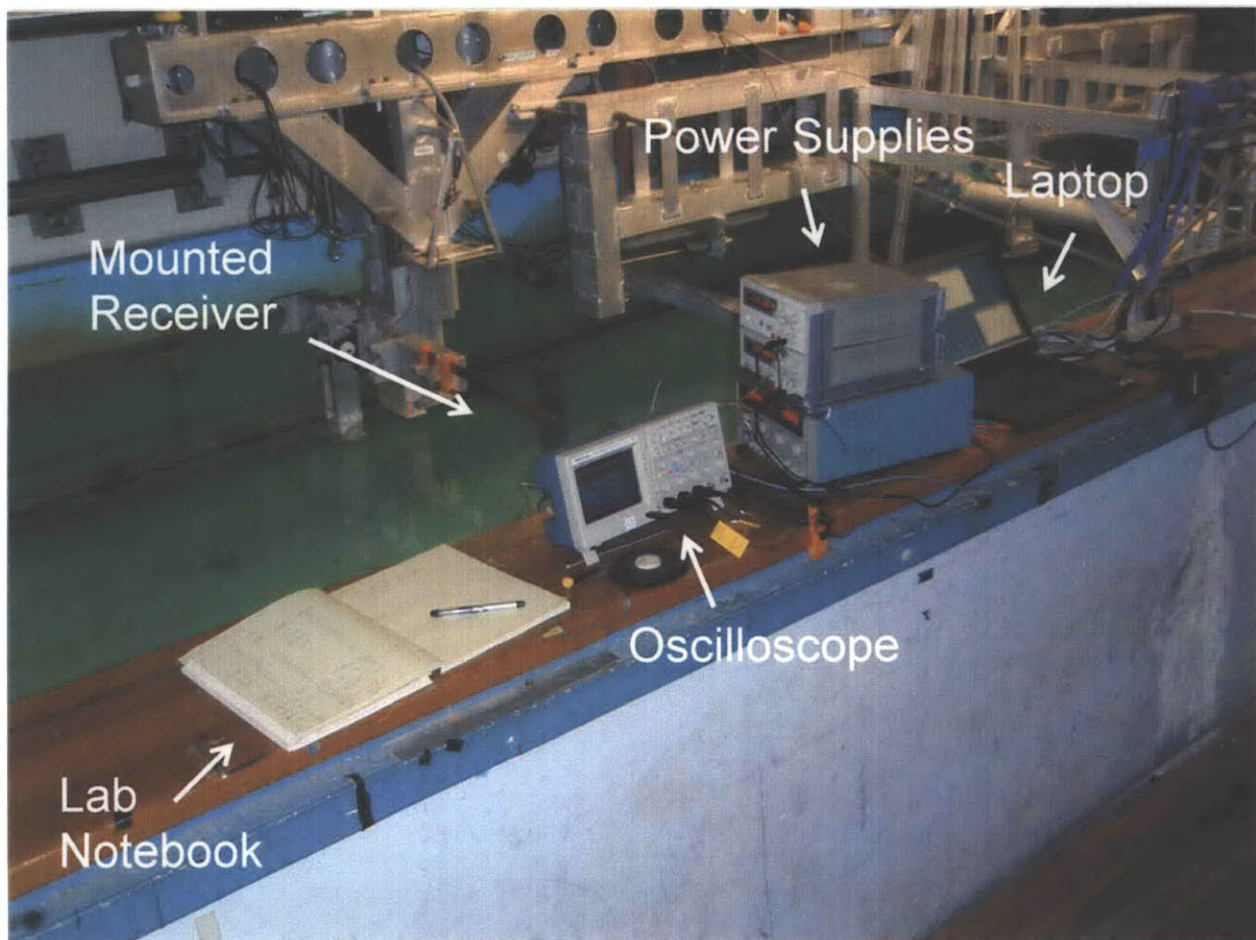


Figure 52 Complete receiver test set-up

4.1.3 Alignment

Once the receiver and transmitter were both mounted, they had to be aligned. This was done by eye and using simple measurements to begin with. You can see the process in Figure 53. First, the transmitter was brought very close to the receiver (a) and the distance below the water level was measured to make sure each optical component was at the same depth. Then a signal was sent through the system to ensure that the transmitter and receiver were aligned well enough to successfully transfer a file (b). By eyeballing where the center of the transmission beam was aimed, slight adjustments to the angle and position of the transmitter were made in an effort to best align the two components (c). Using the oscilloscope, the relative strength of the signal received at the same transmission distance but different alignments could help determine the optimal alignment. As the transmitter was moved further away from the receiver, slight errors in alignment would become more apparent, so occasionally the alignment would be checked by trying to find an alignment that gave a maximum signal.

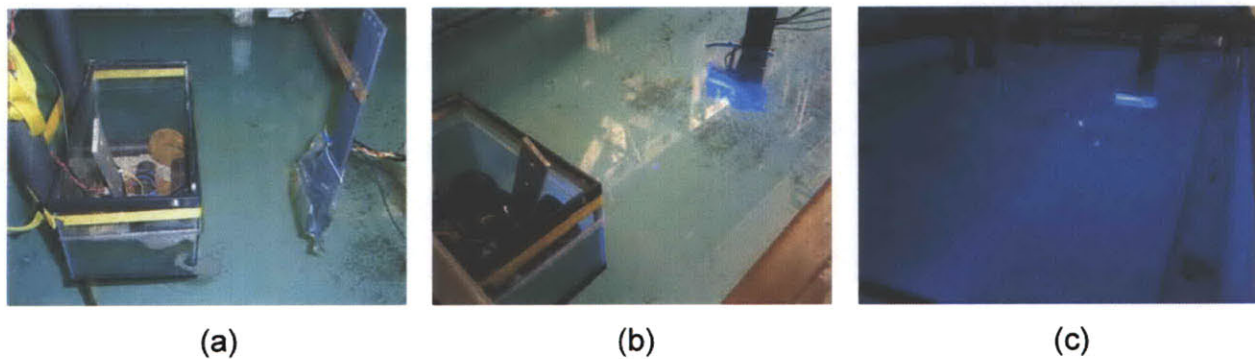


Figure 53 Aligning the transmitter and receiver

4.2 Testing

In order to test the robustness of the system, a signal was sent between the transmitter and receiver at different distances and different transmission speeds. Tests were performed with the lights off to better simulate deep ocean conditions, but many emergency lights could not be turned off, so some ambient light was present during the tests.

A python program (see Appendix) was used to set the transmission speed and push the binary data via the serial port to the transmitter. Another python program (see Appendix) was used to read in the serial data on the receiver side and save it as a file. There was no error checking or handshaking used in the programs. Data was purely pushed out one on end and read in at the other. This means that though the system hardware could successfully send a clean data, sometimes the received file would have errors in it due to a few individual bytes of data being lost in transmission.

The transmission speeds that could be tested were limited to a maximum of 3 Mbps by the USB-TTL converter cable discussed in section 3.1.3. Additionally, the speeds and capabilities of the laptops used to send and receive the data affected how many byte errors were present in the final received file. Tests were performed to better understand the limitations of the laptops and USB-TTL converter cable by connecting the two cables directly to each other (without the optical transmission system in between) and sending files between the two computers (see Figure 54).



Figure 54 Testing sending/receiving capabilities without the optical link

It was observed that though the laptops and cables could successfully send and receive files at 1 Mbps, bytes were lost as speeds increased to 2 and 3 Mbps. This can be seen in Figure 55, where (a) was sent at 1 Mbps and has no loss, (b) was sent at 2 Mbps and shows some errors, and (c) was sent at the maximum of 3 Mbps and shows more errors. This data loss could be due to a number of things, including the buffer size and processing speed of the laptops. Since the test system, without the wireless optical component, cannot successfully send complete files at speeds faster than 1 Mbps without losing some bytes of data, it can't be expected that the test system, with the wireless optical system in place, will be able to do so. For this reason, tests at higher than 1 Mbps done with the optical system relied on viewing the signal received on the

oscilloscope and checking that the beginning of the file was received correctly – showing that transmission of data can be successful at those speeds – instead of comparing the entire received file.

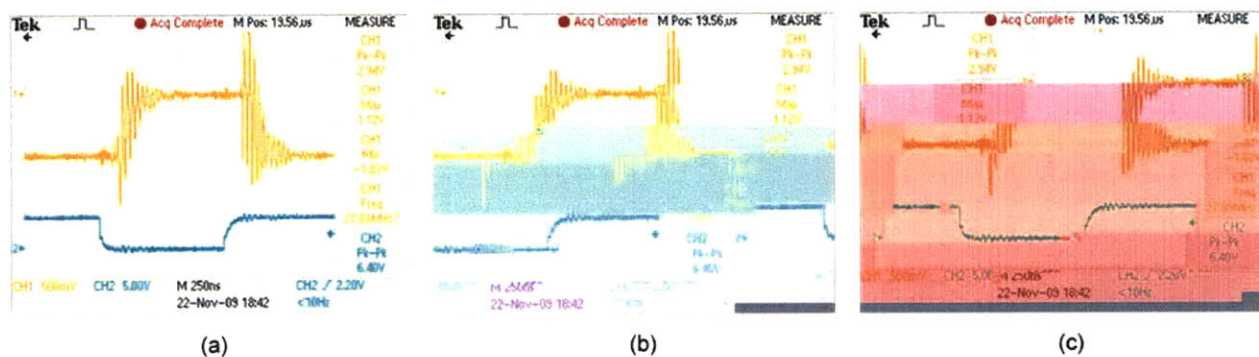


Figure 55 30 KB JPEG file transmitted through cable (a) 1 Mbps (b) 2 Mbps (c) 3 Mbps

4.3 Results

As was expected, the received signal dropped off exponentially as the transmitter was moved further from the receiver. Figure 56 demonstrates this by graphing the voltage level of the output of the transimpedance amplifier at different transmission distances.

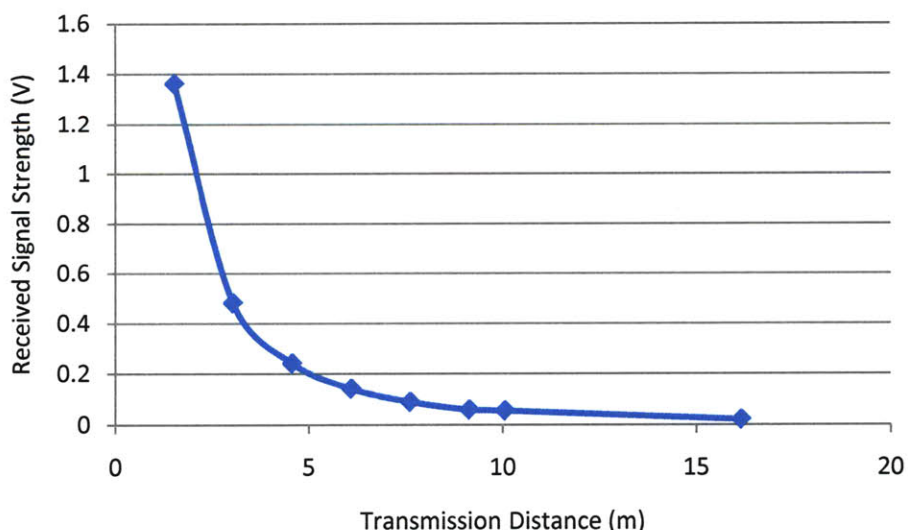


Figure 56 Graph of received signal strength at various transmission distances

Even though the received signal was very low at long distances, the amplification and comparator stages were enough to enable successful transmission at up to 13 meters. Figure 57 shows the received data signal. Trace 1 (orange) is the output of the transimpedance amplifier, trace 2 (blue) is the output of the voltage amplifier, and trace 3 (purple) is the output of the comparator.

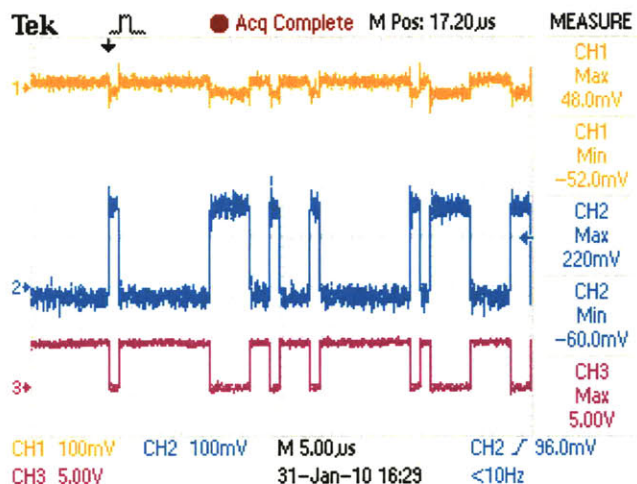


Figure 57 Received data at 1 Mbps over 13 meters

You can see that the signal coming out of the voltage amplifier (trace 2) is significantly larger (about 150 mV) compared to the noise (about 25 mV). This implies that successful transmission could happen over even longer distances. Unfortunately, the reference voltage for the comparator was set to 100 mV (see blue arrow on the right side of trace 2 in Figure 57), so when the distance was a little longer than 13 meters, but less than 16 meters, the reference voltage is just about where the signal voltage is, making the comparator unstable (see Figure 58 (a)). Once 16 meters was reached, the signal voltage from the voltage amplifier dropped below the reference voltage, regaining a clean signal, but not triggering the comparator (see Figure 58 (b)). Since the noise level is in the 25 mV range, the reference voltage could probably be dropped as low as 50 mV, giving a transmission range of at least 16 meters and possibly up to 20 meters.

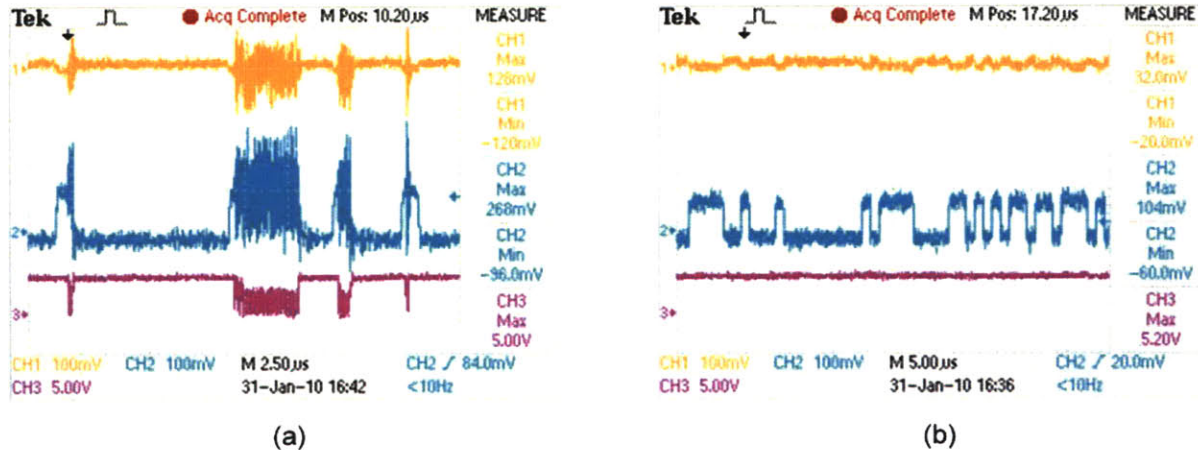


Figure 58 Testing at the distance limits of the system (a) 15 meters (b) 16.2 meters

Multiple data files were successfully transmitted through the optical link at 1 Mbps over 10 meters to demonstrate not only that the signal was clean, but that it could be successfully read by the computer. These files ranged in size 8 KB to 7 MB, and were .txt, .jpg, and .mp3. Just like the tests done between the two computers without the optical system in place, tests done with the optical system in place above 1 Mbps lost bytes in the transmission of the entire file. This was due to the receiving computer and software, not the optical communication system. Figure 59 shows the original 273 KB JPEG file (a) as it was received through the optical link at 1 Mbps (b) and 3 Mbps (c) over 10 meters. Though the 1 Mbps file was received perfectly, the 3 Mbps image is obviously missing data, just as in the control case without the optical link in place. You can see that the beginning of the file was successfully transmitted and received correctly by looking at the first row of pixels.

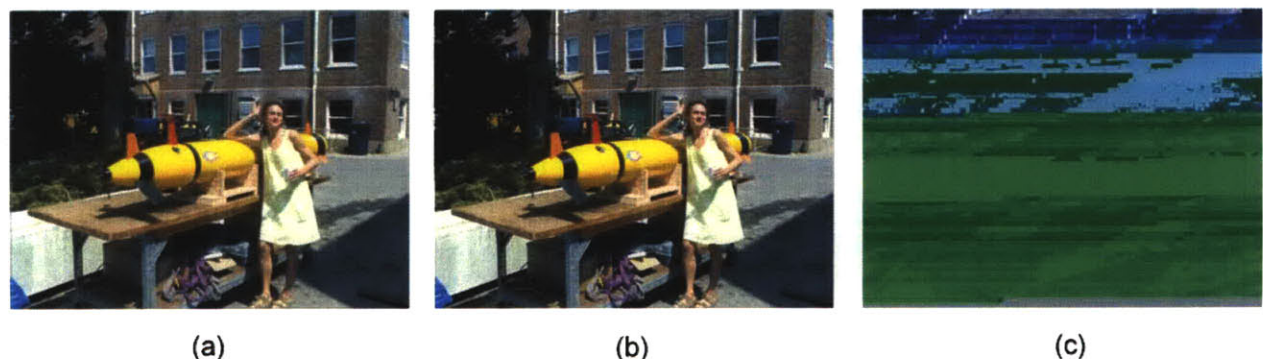


Figure 59 (a) Original file (b) transmitted at 1 Mbps and (c) 3 Mbps over the optical link

Due to the limitations of the testing scenario, it is more appropriate to judge the optical system's ability to transmit and receive a file at high speeds by looking at the actual signals received and processed by the optical receiver instead of the files saved by the computer. Figure 60 shows these signals for a transmission distance of 10 meters. Again, trace 1 (orange) is the output of the transimpedance amplifier and trace 2 (blue) is the output of the voltage amplifier. Unfortunately, during these tests, the reference voltage of the comparator was set at 5 volts, so the signal was not strong enough to trigger the comparator (trace 3 – purple). You can see from the output of the voltage amplifier, however, that the signal is strong even at 3 Mbps.

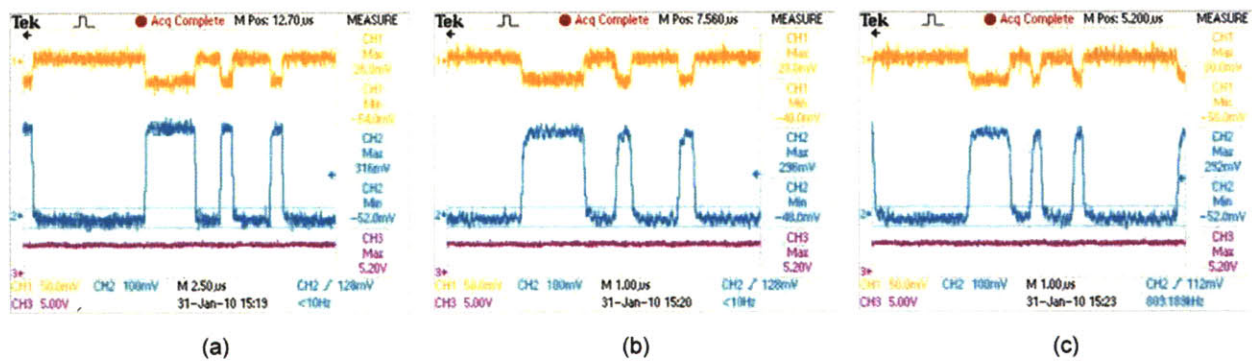


Figure 60 Received data signal at (a) 1 Mbps (b) 2 Mbps (c) 3 Mbps

At the end of the testing, it was noticed that the fish tank that was keeping the transmitter dry had many bubbles on the face of the glass, which could have impacted the transmission of light (see Figure 61). Additionally, it was known that a scratched up plastic bag is a less than ideal waterproof window for the optical receiver. More transparent waterproof housings for the transmitter and receiver would reduce the amount of attenuation and could possibly result in greater transmission distances.

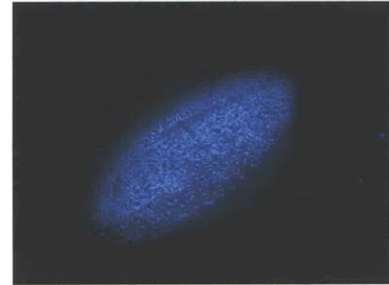


Figure 61 Bubbles on the face of the glass in front of the transmitter

5 Conclusion

Using the test conditions, entire files could be sent with no errors at speeds of 1 Mbps, over distances of 13 meters. Data was shown to be successfully transmitted at speed up of to 3 Mbps, though large files could not be sent without some loss due to the buffer size and processing speed of the laptops used for testing and the lack of error checking in the testing software. Limitations due to the test set-up prevented testing at higher data rates and significant off-axis testing. Better computer software and hardware could enable higher testing speeds and error checking to provide for larger file transfer at higher speeds. Better waterproof housing and less ambient light noise could enable further transmission distances by increasing the signal to noise ratio. Overall, the system performed above expectations, showing speeds of over 1 Mbps at distances over 10 meters. These specifications are more than enough for the scenario, though further testing is desired to characterize off-axis performance and ambient light robustness. This system shows that LED-based wireless optical communication systems are a viable solution to high speed, moderate distance data transmission applications.

6 Bibliography

1. Autonomous Underwater Vehicle. *Wikipedia*. [Online] [Cited: December 18, 2009.] http://en.wikipedia.org/wiki/Autonomous_underwater_vehicle.
2. ROV Background. *Remotely Operated Vehicle Committee of the Marine Technology Society*. [Online] [Cited: December 18, 2009.] <http://www.rov.org/info.cfm>.
3. **Robinson, Stephen.** *Underlying physics and mechanisms for the absorption of sound in seawater*. [<http://resource.npl.co.uk/acoustics/techguides/seaabsorption/physics.html>] UK : National Physical Laboratory.
4. **Pierre-Philippe J. Beaujean, Edward A. Carlson, John Spruance, Dion Kriel.** *HERMES – A High-Speed Acoustic Modem for Real-Time Transmission in Port Environment and Very Shallow Water*. IEEE. <http://ieeexplore.ieee.org/stamp/stamp.jsp?arnumber=05151835>.
5. **Link Quest, Inc.** *Underwater Acoustic Modem Datasheet*. [http://www.o-vations.com/uwm_datasheet.pdf] San Deigo, CA : s.n.
6. **EvoLogics GmbH.** R-Series Underwater Acoustic Modems. *Evo Logics*. [Online] <http://www.evologics.de/en/products/acoustics/index.html>.
7. **Wozniak, Bogdan, and Jerzy Dera.** *Light Absorption in Sea Water*. New York, NY : Springer Business + Science Media, LLC, 2007.
8. **Jacobson, Ted.** Phys104 - How Things Work. *University of Maryland Physics Department*. [Online] <http://www.physics.umd.edu/grt/taj/104a/104anotessupps.html>.
9. **Funk, C.J., S.B. Bryant and P.J. Heckman, Jr.** *Handbook of Underwater Imaging System Design*. Ocean Technology Department Navel Undersea Center, July 1972.
10. **Wireless Fibre Systems Ltd.** Seatooth - High Data Rate. *Wireless Fibre*. [Online] 2010. <http://www.wirelessfibre.co.uk/index.php?page=seatooth>.
11. **Bales, James and Chrysostomos Chrysostomidis.** *High-bandwidth, low-power, short-range optical communication underwater*. 9th International Symposium on Unmanned Untethered Submersible Technology, 1995.
12. **Giles, John W. and Isaac N. Bankman.** *Underwater Optical Communications Systems Part 2: Basic Design Considerations*. MILCOM 2005, 2005.
13. *Optical Modem technology for seafloor observatories*. **Farr, N., A. D. Chave, L. Freitag, J. Preisig, S. White, D. Yoerger, and F. Sonnichsen**. Proceedings of the IEEE Oceans 2006, 2006.
14. **Hanson, Frank and Stojan Radic.** *High bandwidth underwater optical communication*. Optical Society of America, January 10, 2008, Applied Optics, Vol. 47.
15. **Ambalux Corporation.** 1013C1 High-Bandwidth Underwater Transceiver Data Sheet. [Online] http://www.ambalux.com/1013_Brochure.pdf.
16. **Schill, F., U. Zimmer, J. Trumpf.** *Visible Spectrum Optical Communication and Distance Sensing for Underwater Applications*. AGRA 2004.
17. **Sanoner, Damien.** *Underwater Wireless Light Communication*. Cambridge, MA : MIT Sea Grant College Program, 2003.
18. **Doniec, M., I. Vasilescu, M. Chitre, C. Detweiler, M. Hoffmann-Kuhnt, D. Rus.** *AquaOptical: A lightweight Device for High-rate Long-range Underwater Point-to-Point Communication*. IEEE Oceans 2009, 2009.
19. **Scherz, Paul.** *Practical Electronics for Inventors*. New York, NY : McGraw-Hill Companies, Inc., 2007. ISBN 0-07-145281-8.

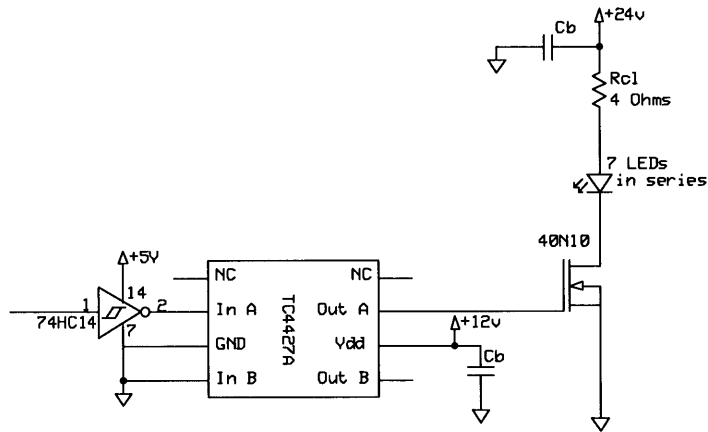
20. **Hranilovic, Steve.** *Wireless Optical Communication Systems*. New York, NY : Springer Science+Business Media, Inc., 2005. ISBN 0-387-22784-9.
21. **Friedman, Edward and John Lester Miller.** *Photonics rules of thumb: optics, electro-optics, fiber optics, and lasers*. USA : McGraw-Hill Professional, 2004. ISBN 0071385193.
22. **Keiser, Gerd.** *Optical Communications Essentials*. USA : McGraw-Hill Companies, Inc., 2003. ISBN 0-07-141204-2.
23. **Gowar, John.** *Optical Communication Systems*. London : Prentice-Hall International, Inc., 1984. ISBN 0-13-638056-5.
24. **Miller, John Lester and Dr. Edward Friedman.** *Optical Communications Rules of Thumb*. USA : McGraw-Hill Companies, Inc., 2003. ISBN 0-07-138778-1.
25. **Moursund, Carter.** *LEDs vs. Laser Diodes for Wireless Optical Communications*. Pasadena, CA : ClearMesh Networks, December 2006.
26. **Philips Lumileds Lighting Company.** Luxeon Rebel PC Amber Data Sheet. 2009.
27. **Lamina Lighting Incorporated.** Titan LED Lighting Engines Data Sheet. 05/21/08.
28. **Fairchild Semiconductor Corporation.** *40N10 Data Sheet*. January 2002.
29. **Microchip Technology, Inc.** *TC4427A Data Sheet*. 2003.
30. **Peacock, Craig.** USB in a NutShell. *Beyond Logic*. [Online] April 6, 2007. [Cited: January 7, 2010.] <http://www.beyondlogic.org/usbnutshell/usb2.htm>.
31. **BEAM Robotics.** Schmitt Inverter. *BEAM Wiki*. [Online] June 30, 2009. [Cited: January 9, 2010.] http://www.beam-wiki.org/wiki/Schmitt_Inverter.
32. **Wikipedia.** Photoconductivity. *Wikipedia*. [Online] January 8, 2010. [Cited: January 10, 2010.] <http://en.wikipedia.org/wiki/Photoconductivity>.
33. **mikroElektronika.** Thyristors, triacs, diacs. *Understanding Electronic Components*. [Online] 2003. [Cited: January 10, 2010.] <http://www.mikroe.com/en/books/keu/06.htm>.
34. **EG&G, Inc.** Choosing the Detector for you Unique Light Sensing Application. *EG&G Optoelectronics*. [Online] 1997. [Cited: January 10, 2010.] <http://www.engr.udayton.edu/faculty/jloomis/ece445/topics/egginc/tp4.html>.
35. **Adrio Communications Ltd.** Phototransistor or photo transistor. *Radio Electroincs*. [Online] [Cited: January 10, 2010.] http://www.radio-electronics.com/info/data/semicond/phototransistor/photo_transistor.php.
36. **Wikipedia.** Photomultipliers. *Wikipedia*. [Online] December 4, 2009. [Cited: January 10, 2010.] http://en.wikipedia.org/wiki/Photomultiplier#Usage_considerations.
37. **Tkachenko, Nikolai V.** *Optical Spectroscopy: methods and insturmentations*. Elsevier, 2006. ISBN 0444521267.
38. **Alexander, Stephen B.** *Optical Communication Receiver Design*. Bellingham, WA : SPIE Optical Engineering Press, 1997. ISBN 0-8194-2023-9.
39. **Pacific Silicon Sensor, Inc.** Silicon Photodiodes. *Pacific Silicon Sensor*. [Online] 2010. [Cited: January 10, 2010.] http://www.pacific-sensor.com/pages/sp_all.html.
40. **Johnston, Davis A.** *Handbook of Optical Through the Air Communications*. [<http://www.imagineeringzine.com/ttaoc/r-circuits.html>] s.l. : Imagineering E-Zine, 2008.
41. **Pease, Robert A.** *What's All This Transimpedance Amplifier Stuff, Anyhow?* <http://electronicdesign.com/article/analog-and-mixed-signal/page/3/what-s-all-this-transimpedance-amplifier-stuff-any.aspx> : Electronic Design, January 8, 2001.
42. **Texas Instruments.** *THS461 Data Sheet*. <http://focus.ti.com/lit/ds/symlink/ths4631.pdf> : March 2005.

43. **National Semiconductor.** *LM7171 Datasheet*.
[<http://www.national.com/ds/LM/LM7171.pdf>] May 2006.
44. **Woodford, Chris.** Semiconductor diode lasers. *Explain that Stuff?* [Online] September 12, 2009. [Cited: January 5, 2010.]
<http://www.explainthatstuff.com/semiconductorlaserdiodes.html>.

Appendix

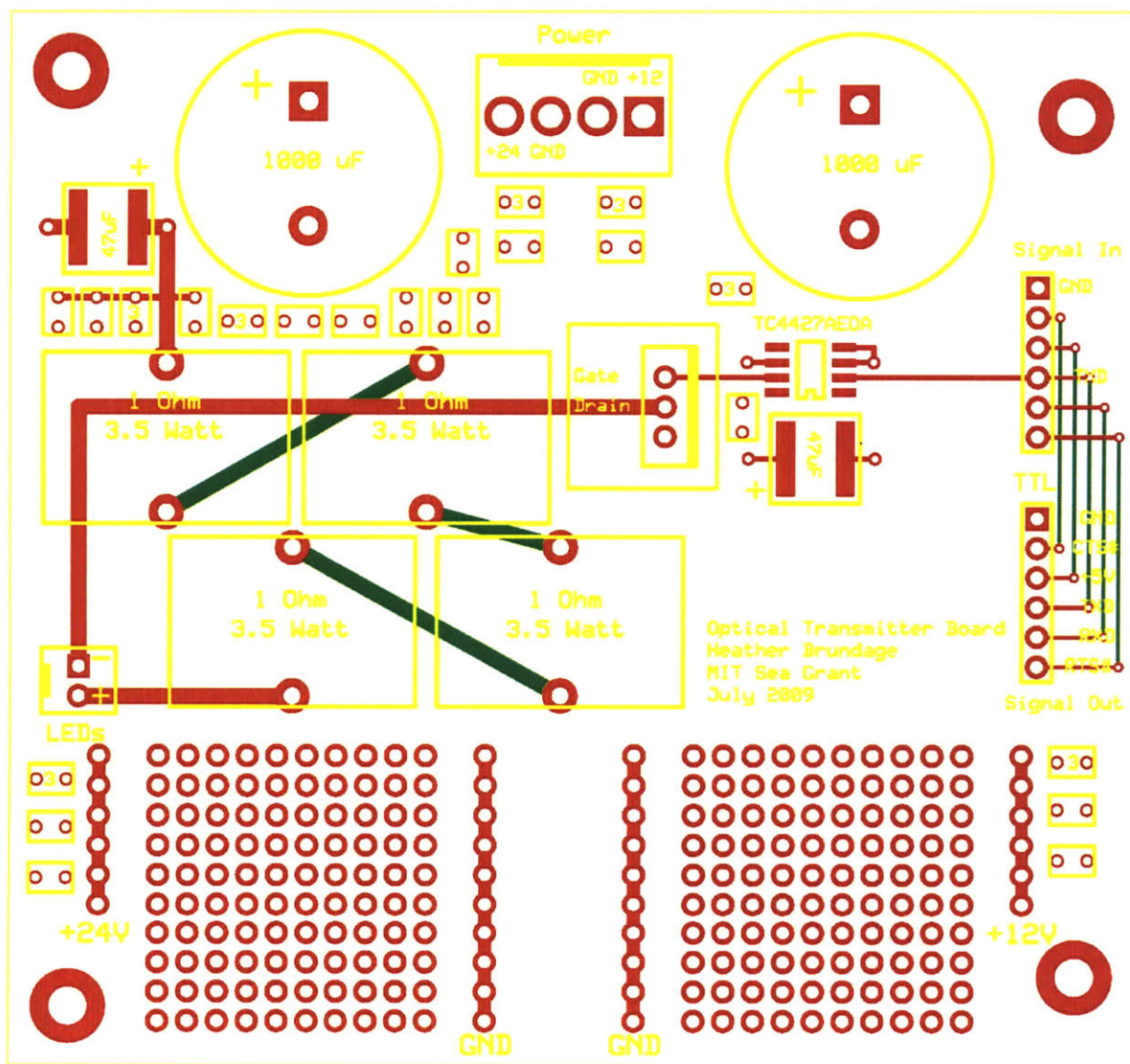
List of Contents

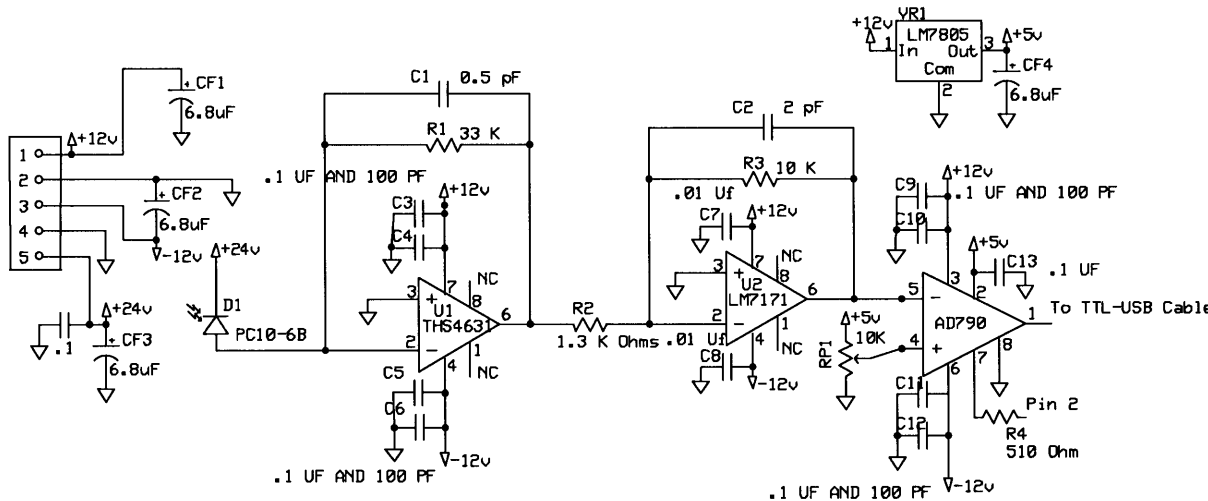
Transmitter Schematic
Transmitter Printed Circuit Board Layout
Receiver Schematic
Receiver Printed Circuit Board Layout
Python scripts for sending and receiving files for testing



Heather Brundage
Transmitter Schematic

MIT Sea Grant	Rev 1.3	Modified PCB
	6/22/2009	

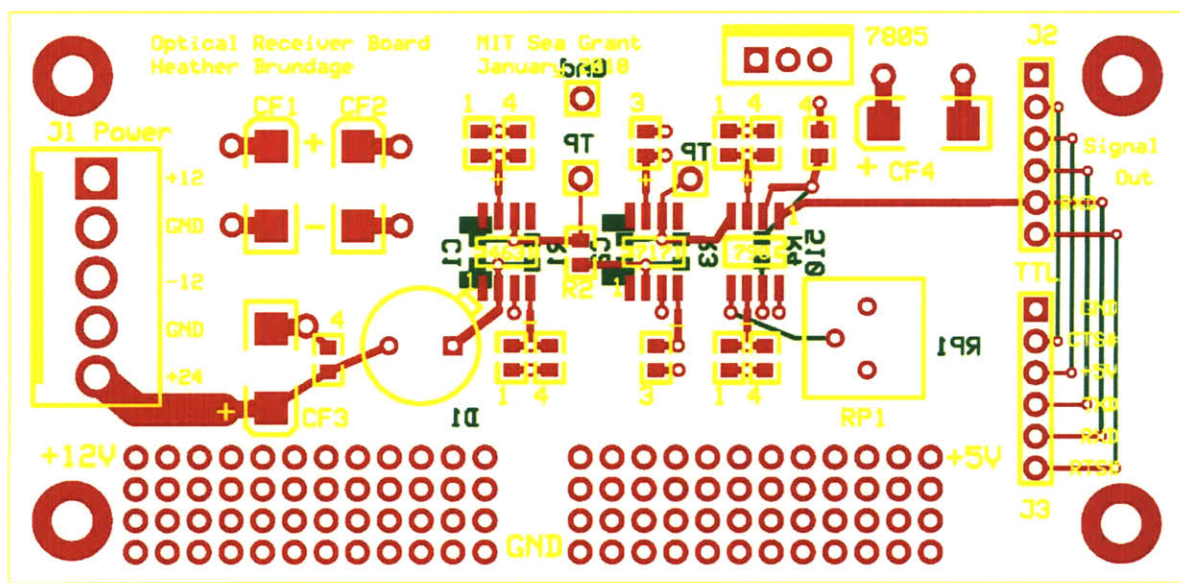




Heather Brundage

Optical Receiver

MIT Sea Grant	Rev 4.0	Final PCB Version
	1/15/2010	



Python script to transmit a file:

```
#!/usr/bin/env python

import serial, sys, time

infile = open("C:\\\\Users\\\\Heather\\\\Desktop\\\\AUV_girl.jpg",'rb')
data = infile.read()
infile.close()

ser = serial.Serial('COM6',1000000)
ser.close()
ser.open()

start_time = time.time()
ser.write(data)
ser.close()
end_time = time.time()
print "Serial write took %02f seconds" % (end_time-start_time,)
```

Python script to receive a file:

```
#!/usr/bin/env python

import serial, sys, time

filesize = 273975
outfile = open("outputTemp.jpg",'wb')

ser = serial.Serial('COM5',3000000,timeout=10)
ser.close()
ser.open()
start_time = time.time()
ser.flushInput()
data=ser.read(filesize)
ser.close()
end_time = time.time()
print "Serial read took %02f seconds" % (end_time-start_time,)

outfile.write(data)
outfile.close()
print "Done."
```